

POLITECNICO DI TORINO

Dipartimento di Ingegneria Meccanica e Aerospaziale
Corso di Laurea Magistrale in Ingegneria Aerospaziale



MSc Thesis

Pitch Control Unit redesign for Additive Manufacturing

Supervisors:

Prof. Carlo Rosso

A handwritten signature in blue ink, appearing to read 'Carlo Rosso', positioned above a dotted line.

Ing. Edoardo Peradotto

A handwritten signature in blue ink, appearing to read 'E. Peradotto', positioned above a dotted line.

Candidate:

Dámaso Luque Arias

A handwritten signature in blue ink, appearing to read 'Damaso Luque Arias', positioned above a dotted line.

A.A 2017/2018

Index

ABSTRACT	1
1. INTRODUCTION	2
1.1. BACKGROUND	2
1.2. PURPOSE	2
1.3. THESIS STRUCTURE	2
2. ADDITIVE MANUFACTURING (AM)	3
2.1. METAL ADDITIVE MANUFACTURING	6
2.1.1. <i>Powder feed systems</i>	7
2.1.2. <i>Wire feed systems</i>	7
2.1.3. <i>Powder bed systems</i>	8
2.2. APPLICATIONS	11
2.3. GENERIC AM PROCESS	12
2.4. MANUFACTURING GUIDELINES FOR METAL AM.....	14
3. STRUCTURAL OPTIMIZATION METHODS	18
3.1. TOPOLOGY OPTIMIZATION.....	18
3.1.1. <i>SIMP method</i>	19
3.2. LATTICE OPTIMIZATION.....	20
3.3. SIZE OPTIMIZATION.....	22
3.4. FREE-SIZE OPTIMIZATION	22
3.5. SHAPE OPTIMIZATION.....	23
3.6. TOPOGRAPHIC OPTIMIZATION	24
3.7. FREE-SHAPE OPTIMIZATION	24
4. PROBLEM DEFINITION: PITCH CONTROL UNIT (PCU)	26
4.1. DESCRIPTION OF THE SYSTEM.....	26
4.1.1. <i>Assembly components</i>	28
4.1.2. <i>Hydraulic valves</i>	30
5. DESIGN OPTIMIZATION	35
5.1. CAD MODELING	35
5.2. FEM ANALYSIS	47
5.2.1. <i>Baseline analysis</i>	47
5.2.2. <i>Dynamic analysis approach</i>	48
5.2.3. <i>Topology optimization</i>	49
5.3. OPTIMIZATIONS	52

5.3.1.	<i>Min mass with lower bound in first mode frequency</i>	53
5.3.2.	<i>Min mass with frf displacement control</i>	54
5.3.3.	<i>Min mass with lower bound in first mode frequency + frf displacement control</i>	55
5.4.	SMOOTHING & SOLUTION REFINEMENT	55
6.	DESIGN VALIDATION	56
7.	FURTHER DEVELOPMENTS	58
8.	CONCLUSIONS	59
I.	APPENDIX A: DYNAMIC ANALYSIS OF A BEAM WITH IMPOSED ACCELERATION.	60
II.	APPENDIX B: EQUIVALENT SELF-SUPPORTING CROSS SECTION	64
	BIBLIOGRAPHY	67

LIST OF FIGURES

FIGURE 1.1 FLOWCHART OF THE STEPS FOLLOWED IN THE REDESIGN OF THE COMPONENT [1].	3
FIGURE 2.1 HYPE CYCLE FOR 3D PRINTING IN 2014 [4].	6
FIGURE 2.2 HYPE CYCLE FOR 3D PRINTING IN 2015 [4].	6
FIGURE 2.3 GENERIC ILLUSTRATION OF AN AM POWDER FEED SYSTEM, FROM [2].	7
FIGURE 2.4 ILLUSTRATION OF AN AM WIRE FEED SYSTEM WITH ELECTRON BEAM ENERGY SOURCE [5].	8
FIGURE 2.5 GENERIC ILLUSTRATION OF A POWDER BED FEED SYSTEM [2].	8
FIGURE 2.6 LOCALIZATION OF THE TECHNOLOGIES FOR POWDER BED FUSION METAL ADDITIVE MANUFACTURING.	9
FIGURE 2.7 SPECTRA H MACHINE FROM ARCAM, THE NEWEST MACHINE IN THE EBM FIELD [7].	10
FIGURE 2.8 CONCEPT LASER XLINE 2000R [8].	10
FIGURE 2.9 STL FORMAT TEMPLATE TO DEFINE A SINGLE TRIANGLE.	12
FIGURE 2.10 PRE- AND POST-PROCESSED PART PRINTED WITH AM.	13
FIGURE 2.11 EFFECT OF DIAMETER IN LATERAL HOLES.	15
FIGURE 2.12 STAIRCASE EFFECT.	16
FIGURE 2.13 ORIENTATION OF THE PART WITH RESPECT TO THE RECOATER IS IMPORTANT.	17
FIGURE 2.14 RESIDUAL STRESS AFTER MELTING THE POWDER LAYER [12].	17
FIGURE 3.1 TOPOLOGY OPTIMIZATION.	19
FIGURE 3.2 EFFECT ON THE DENSITY VALUE FOR DIFFERENT VALUES OF THE PENALIZATION PARAMETER.	20
FIGURE 3.3 LATTICE OPTIMIZATION EXAMPLE WHERE THE LOAD DISTRIBUTION BETWEEN LATTICE ELEMENTS IS OPTIMIZED [13].	21
FIGURE 3.4 EXAMPLES OF DIFFERENT TYPE OF LATTICES AVAILABLE DEPENDING ON THE TYPE OF SOLID ELEMENT REPLACED [13].	22
FIGURE 3.5 RANGE OF THE VALUES THAT THICKNESS CAN ADOPT IN THE FREE-SIZE OPTIMIZATION.	22
FIGURE 3.6 FREE-SIZE OPTIMIZATION.	23
FIGURE 3.7 SHAPE OPTIMIZATION.	23
FIGURE 3.8 TOPOGRAPHIC OPTIMIZATION.	24
FIGURE 3.9 FREE SHAPE OPTIMIZATION OF A CLAMPED BEAM. THE DESIGN REGIONS ARE THE VERTICAL OUTER SURFACES OF THE BEAM.	25
FIGURE 4.1 PROPELLER MECHANISM TO GET A PITCH VARIATION FROM THE BETA TUBE [15].	26
FIGURE 4.2 OPERATING SCHEME OF A GENERIC PCU [16].	27
FIGURE 4.3 SCHEME OF THE ASSEMBLY OF THE PCU.	27
FIGURE 4.4 REAR VIEW OF THE ASSEMBLY.	28
FIGURE 4.5 MAIN BODY OF THE PCU SCHEMATIZED.	29
FIGURE 4.6 MID-HOUSING (GREEN) AND BETA FEEDBACK TRANSDUCER (ORANGE) SCHEMATIZED.	30
FIGURE 4.7 SCHEMATIZED ELECTRICAL CONNECTORS OF THE VALVES. ALL OF THEM ARE BOLTED TO THE MAIN BODY.	30
FIGURE 4.8 SCHEME OF A SOLENOID VALVE.	31
FIGURE 4.9 SCHEME OF A SPOOL VALVE.	31
FIGURE 4.10 OPERATION SCHEME OF A SERVO VALVE.	32
FIGURE 4.11 SCHEME OF A NON-RETURN VALVE.	32
FIGURE 4.12 THE EFFECT OF D/D RATIO ON STRESSES FOR PLUG AND BOSS MATERIAL WITH SIMILAR MECHANICAL PROPERTIES. [17].	33
FIGURE 4.13 EFFECT OF D/D RATIO ON PLUG AND BOSS DISSIMILAR MECHANICAL PROPERTIES. [17].	33

FIGURE 5.1 THE DESIGN PROCESS SIMPLIFIED.	35
FIGURE 5.2 EXTERNAL PROFILE OF THE VALVES AND CONNECTOR INTERFACES TO MAINTAIN IN THE REDESIGN.	36
FIGURE 5.3 POSSIBLE CONCEPTUAL LAYOUTS. FRONTAL VIEW OF PROPOSAL 3.	36
FIGURE 5.4 PROPOSAL 4 FOR POSSIBLE CONCEPT OF LAYOUTS.	37
FIGURE 5.5 PROPOSAL 5 FOR POSSIBLE CONCEPTUAL LAYOUTS.	37
FIGURE 5.6 PROPOSAL 6 FOR POSSIBLE CONCEPTUAL LAYOUTS.	38
FIGURE 5.7 PROPOSAL 7 FOR POSSIBLE CONCEPTUAL LAYOUTS.	38
FIGURE 5.8 PROPOSAL 7 3D CAD MODEL WITHOUT THE WRAPPING SHELL FOR THE OIL DRAIN SUMP.	39
FIGURE 5.9 PROPOSAL 8 FOR POSSIBLE CONCEPTUAL LAYOUTS.	39
FIGURE 5.10 SECTION TO ILLUSTRATE THE CONCEPT OF SHARED HOLE DIRECTLY PRINTED WITHIN THE BODIES OF THE VALVES.	40
FIGURE 5.11 PROPOSAL 9 FOR POSSIBLE CONCEPTUAL LAYOUTS.	40
FIGURE 5.12 DETAIL OF THE SECTION FOR SOME OIL LINES ATTACHED TO THE BODY OF A VALVE TO SAVE PRINTING SUPPORTS.	41
FIGURE 5.13 PROPOSAL 10 FOR POSSIBLE CONCEPTUAL LAYOUTS. DEFINITIVE CAD SOLUTION ADOPTED.	41
FIGURE 5.14 ISO VIEW OF THE CAD CONCEPT.	42
FIGURE 5.15 DETAIL OF THE DRAINING OF ONE OF THE VALVES DIRECTLY TO THE ENCLOSED VOLUME BY THE SHELL.	42
FIGURE 5.16 FRONT VIEW OF THE CAD CONCEPT.	43
FIGURE 5.17 LATERAL VIEW OF THE CAD CONCEPT.	43
FIGURE 5.18 REAR VIEW OF THE CAD CONCEPT.	44
FIGURE 5.19 DETAIL OF THE SECTION OF THE SEALING RADIAL O-RING SOLUTION ADOPTED.	45
FIGURE 5.20 AXIAL SEALING O-RING OPTION.	45
FIGURE 5.21 RADIAL O-RING TO SEAL THE INTERFACE BETWEEN MID-HOUSING AND THE MAIN BODY. A VARIANT OF FIRST OPTION WAS ADOPTED.	46
FIGURE 5.22 FINAL CAD SOLUTION ADOPTED. NOTICE THE NEW POSITION OF CONNECTORS TO IMPROVE ENGINE ASSEMBLY OPERATIONS.	47
FIGURE 5.23 SHAKER TABLE AS THE ABSOLUTE REFERENCE.	48
FIGURE 5.24 EXTERNAL NON- INERTIAL ABSOLUTE REFERENCE.	49
FIGURE 5.25 NON-DESIGN SPACE MESHED.	50
FIGURE 5.26 DESIGN SPACE VERSION 1.	50
FIGURE 5.27 DESIGN SPACE VERSION 2.	51
FIGURE 5.28 DESIGN SPACE VERSION 3 WITH THE EDGES AT 45°.	52
FIGURE 5.29 FIRST FREQUENCY CONSTRAINED TO THE MAX FREQUENCY OF TEST (LEFT) AND THE MAX FREQUENCY PLUS A 15% MARGIN (RIGHT). DENSITY THRESHOLD >0.7.	53
FIGURE 5.30 FREQUENCY RESPONSE DISPLACEMENTS CONSTRAINED TO A REFERENCE VALUE. LEFT: LOW STRUCTURAL DAMPING RATIO. RIGHT: FIVE TIMES HIGHER STRUCTURAL DAMPING RATIO.	54
FIGURE 5.31 DETAIL OF SUPPORT BUILT CASUALLY BY OPTIMIZATION.	55
FIGURE 5.32 RESULTING DESIGN SPACE AFTER THE SMOOTHING WITH THE SOFTWARE TOOL.	56
FIGURE 5.33 DETAIL OF A ZONE BEFORE (RIGHT) AND AFTER (LEFT) THE SMOOTHING PROCESS.	56
FIGURE 6.1 FIRST MODAL DEFORMED SHAPE OF THE OPTIMIZED CONCEPT	57
FIGURE I.1 CLAMPED BEAM MODEL ANALYZED.	60

FIGURE I.2 GRAV (LEFT) AND SPCD (RIGHT) APPROACHES SCHEMATIZED.	61
FIGURE I.3 GRAV APPROACH. ACCELERATION RESPONSE MEASURED IN THE CLAMP OF THE BEAM.....	61
FIGURE I.4 SPCD APPROACH. ACCELERATION RESPONSE MEASURED IN THE CLAMP OF THE BEAM.	62
FIGURE I.5 GRAV (TOP) AND SPCD (BOTTOM) APPROACHES. ACCELERATION RESPONSE (MAGNITUDE AND PHASE) MEASURED IN THE TIP OF THE BEAM.....	63
FIGURE II.1 SKETCH FOR THE DEFINITION OF GEOMETRIC PARAMETERS.....	64
FIGURE II.2 DIFFERENCE OF RADIUS BETWEEN SECTIONS WITH THE SAME AREA. LEFT: TEARDROP; RIGHT: CIRCULAR.	66

Abstract

The objective of this thesis is to optimize an existing design of a hydraulic component exploiting the potential of additive manufacturing technologies. Indeed, the evolution of additive manufacturing (AM) has opened the opportunity of combination with structural optimization techniques such as topology optimization to develop new designs lighter, cheaper and more efficient.

During this thesis work the candidate has had the opportunity to assist to the development of every phase of the design process, which goes from the identification of suitable candidates for AM, to the exploration of different concepts, then the design of the definitive concept, and eventually the consecution of the topology optimization and the geometry reconstruction from the optimization results with a view to a future printing in an AM machine. In conclusion, a highly recommendable and transversal experience for the figure of modern designer, able to interact with and manage each design phase.

The thesis first presents a classification of the various technologies for AM, focusing more in the powder bed fusion of metals. These technologies are likely to replace some of the classic manufacturing processes and a balance with advantages and disadvantages is made. Subsequently, different types of structural optimization are presented as they are likely to be combined with AM. From all the available options presented, topology optimization is applied to the case study. The main driver for optimization has been to reduce mass with maintained or even improved mechanical properties as a constraint. This has been combined as well with design guidelines for AM to respect the manufacturing limiting parameters.

Structural optimization has demonstrated to be an outstanding tool in the design process. Nevertheless, it is still the designer's task to assess and interpret the results from optimization to identify the most effective application of these techniques, while obviously as in every structural analysis, to apply loads and boundary conditions properly making the correct considerations.

1. Introduction

This Master Thesis work intends to give an idea of all the potentialities of the new generation of manufacturing technologies spreading along with the so called Industrial 4.0 revolution, in which design is not constrained to conventional manufacturing techniques and more space for creativity and design freedom is left to think of more efficient, lighter and robust parts to face the challenges of industry for the coming decades.

In particular, the case study developed in the following pages brings a clear example of component redesign opportunity, in which an extensive use of conventional manufacturing operations is currently made, and by extracting its conceptual functionalities a totally new design is conceived with less manufacturing constraints than its predecessor.

1.1. Background

The thesis work has been developed in collaboration with Avio Aero, a GE Aviation business that within the last years has become a top-class supplier of innovative technological solutions to quickly respond to the endless changes required by the market. A mention apart deserves the efforts made in the field of additive manufacturing, identified as one of the driving technologies of the future industry and the technology where Avio Aero has been investing at. The first example is the inauguration in 2013 in Cameri (Italy) of one of the largest plants in the world dedicated exclusively to the manufacturing of parts by additive manufacturing. Also, Avio Aero has recently involved university to push forward the knowledge in the technology with the launch of an R&D project with the opening in 2017 of the Turin Additive Laboratory (TAL).

1.2. Purpose

Identify and execute new design opportunities thanks to the use of additive manufacturing. Successively, a phase of optimization is begun in order to combine additive with topology optimization exploiting all the synergies between them.

1.3. Thesis structure

By looking to the literature, one could choose from a broad variety of methodologies to tackle the problem, but the flowchart followed in [1] was considered the one that sticks better to the case study of this thesis. See the flowchart reported in the fig. 1.1.

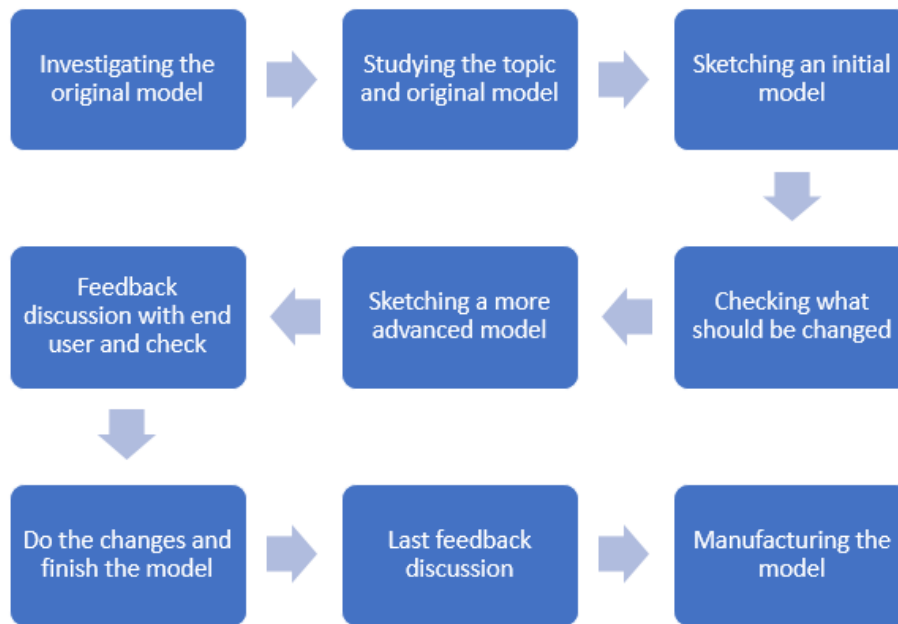


Figure 1.1 Flowchart of the steps followed in the redesign of the component [1].

Moreover, the methodology that can be followed to face problems related to topology optimization can be identified with the following steps:

- 1) Problem definition
- 2) Design optimization
- 3) Design validation

2. Additive manufacturing (AM)

We could take as a generic definition for additive manufacturing the one proposed by the ASTM, describing this technology as “a process of joining materials to make objects from 3D model data, usually layer upon layer, as opposed to subtractive manufacturing methodologies. Synonyms: additive fabrication, additive processes, additive techniques, additive layer manufacturing, layer manufacturing and freeform fabrication” [2].

Compared to conventional, subtractive methods, AM provides the possibility for parts of incredible geometrical complexity, without any impact on direct manufacturing cost. Furthermore, AM may eliminate the need for tooling and reduce the number of production and assembly steps.

On the other hand, build rates are much lower, the production is typically not scalable, component size is limited to the build chamber size, the material properties are only partly controlled, and surface finish and dimensional accuracy are generally below to those obtained with conventional methods making the post processing still necessary.

Different types of techniques can be identified depending on material used (plastic, metal, ceramic) and the material feed method (wire, powder, deposition). One classification scheme that can be used to understand the world of additive manufacturing can be found in [3], where the technologies are separated into groups where processes which use a common type of machine architecture and similar materials transformation physics are grouped, giving as a result the table 3.1. This classification was adopted by the ASTM F42 committee for Additive Manufacturing to distinguish between additive technologies.

Process Type	Technique definition	Example technology	Material available
Vat Photopolymerization	Liquid photopolymer in a vat is selectively cured to form the desired cross-section.	Stereo lithography (SLA), digital light processing (DLP)	Polymers and ceramics
Material Jetting	Droplets of build material are selectively deposited.	3D inkjet printing	Polymers and composites
Binder Jetting	Liquid bonding agent is selectively deposited to join powder materials.	3D inkjet printing	Metal, polymers and ceramics
Material Extrusion	Material is selectively dispensed through a nozzle that scans following the part cross-section.	Fused deposition modelling (FDM)	polymers
Powder bed Fusion	Thermal energy (laser, electron beam) selectively fuses regions of a powder bed.	Selective laser sintering (SLS), Selective laser melting (SLM), electron beam melting (EBM)	Metal, polymer, composites and ceramics
Sheet Lamination	A process in which material is in sheet form and layers of material are deposited and bonded.	Ultrasonic Consolidation (UC)	Hybrids, metals and ceramics
Directed Energy Deposition	Focused thermal energy fuses materials simultaneously by melting as the material is being deposited.	Laser material deposition (LMD)	Metals and hybrid metals

Table 2.1 AM technologies, as classified by ASTM F42 Committee for Additive Manufacturing.

The evolution of additive as a technology is well known and has been monitored through the last years, being identified as one of the most promising candidates for the next revolution in the industry, together with trends such as big data and digital industry. Certainly, the additive industry has evolved from being a promising concept generating many expectations to represent a true alternative for some industrial sectors. The next challenges are to become a real option to be considered and to evolve towards a more productive technology to settle definitively. One example to appreciate the evolution of the additive during years are the hype curves for the 3D printing

market released by [4] in 2014 and 2015, in where the advance of the technology is appreciated and close to reach its point of maturity in the next 5 -10 years.

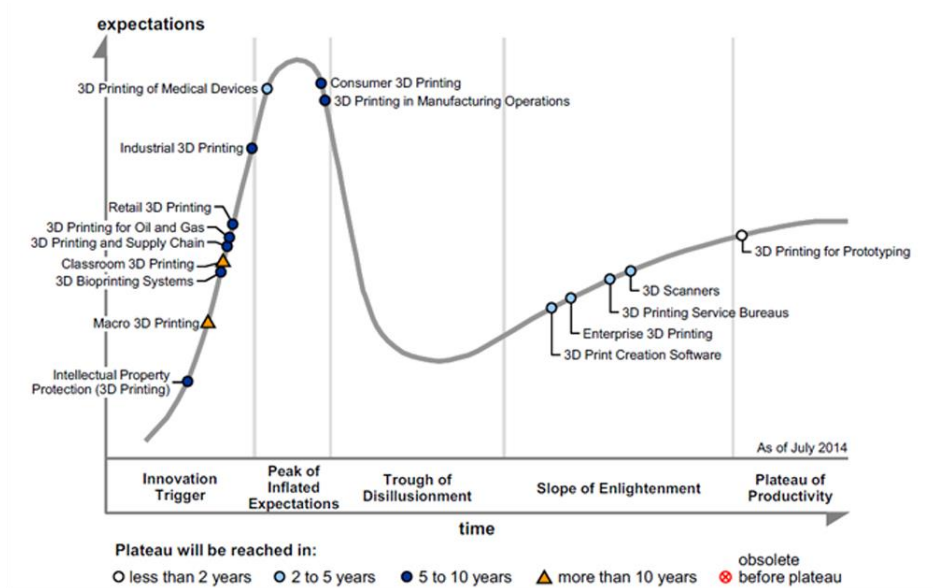


Figure 2.1 Hype cycle for 3D printing in 2014 [4].

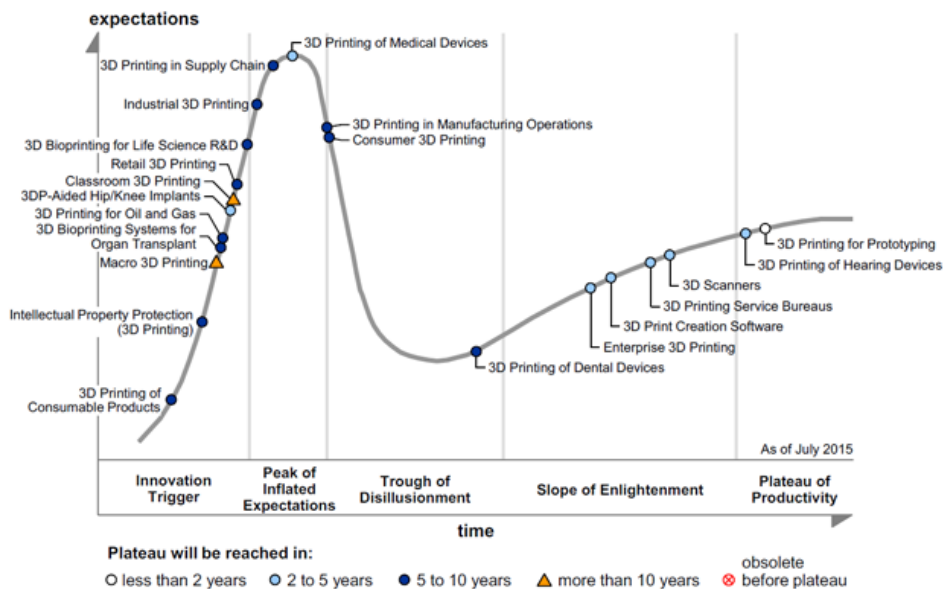


Figure 2.2 Hype cycle for 3D printing in 2015 [4].

2.1. Metal additive manufacturing

One of the areas of commercial interest of AM developed recently is the metal additive manufacturing. The manufacturing systems for this type of AM could be divided into three broad categories: powder bed systems, powder feed systems and wire feed systems. A brief remark will be made of the two latter, while the powder bed systems will be more developed due to their importance in the market share of the sector.

Indeed, most direct metal AM systems work using point-wise method and nearly all of them utilize metal powders input. Furthermore, recent improvements in laser technology, machine accuracy, speed and cost have opened up this market, making many big companies like GE to turn their eyes to considering these processes as promising for the future of the industry.

2.1.1. Powder feed systems

In these systems powder is conveyed through a nozzle onto the build surface. A laser is used to melt a monolayer or more of the powder into the shape desired.

Also known as Direct Energy Deposition (DED) methods, this approach allows the process to be used to add material to an existing part making this option very attractive to repair expensive metal components. The material is jetted along with the laser, making a very efficient use of the powder. Another advantage of this method includes its larger build volume (e.g. $>1.3 \text{ m}^3$ for the Optomec LENS 850-R unit).

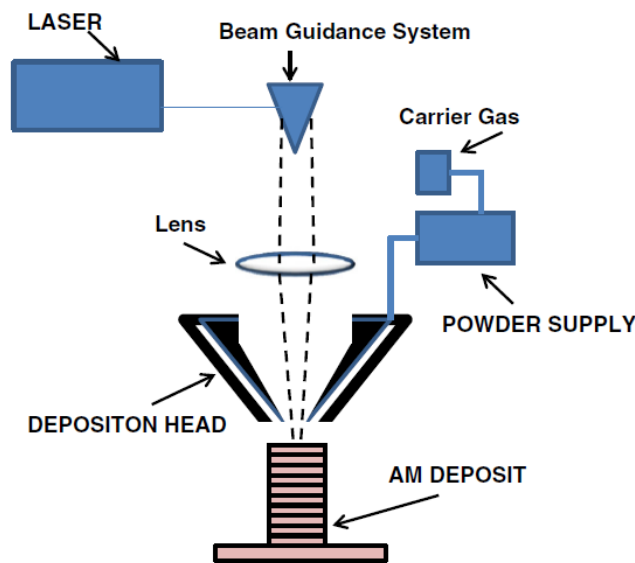


Figure 2.3 Generic illustration of an AM powder feed system, from [2]

2.1.2. Wire feed systems

The wire feed systems use as a source of material a solid wire of metal, positioning in the right place before the energy beam (electron beam, laser beam, or plasma arc) melts the wire, achieving a very high efficiency of material deposition. In fact, wire feed methods are specially indicated for high deposition rate processing and have large build volumes. On the other hand, the fabricated product usually requires more extensive machining than the powder bed or the DED systems do.

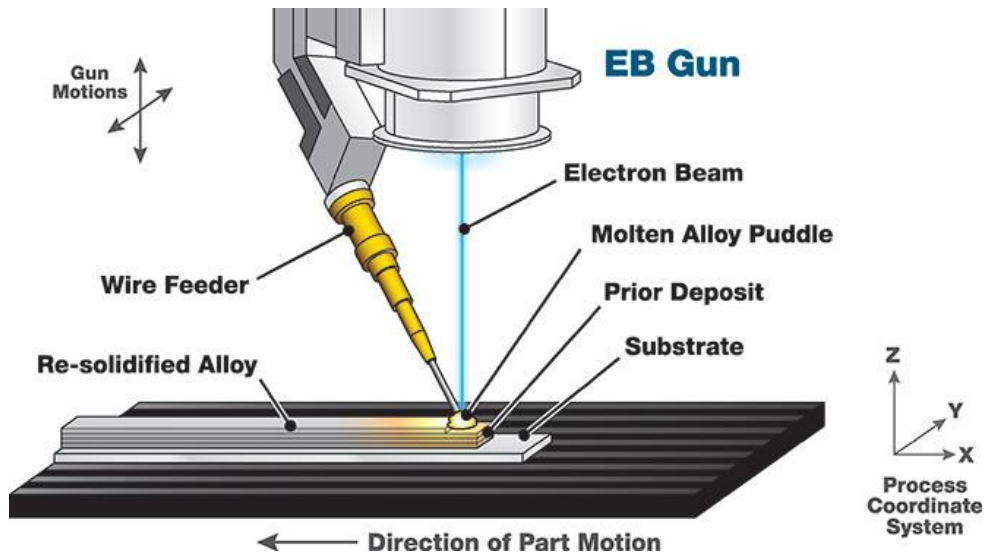


Figure 2.4 Illustration of an AM wire feed system with electron beam energy source [5].

2.1.3. Powder bed systems

These systems create a powder bed by raking or rolling powder fed from the cassettes into a compacted layer usually several powder particles thick, which is then selectively melted by the scanned electron or laser beam. These powders are rapidly solidified or atomized in an inert environment such as purified argon (DMLS, DMLM technologies) or directly vacuum (EBM technology).

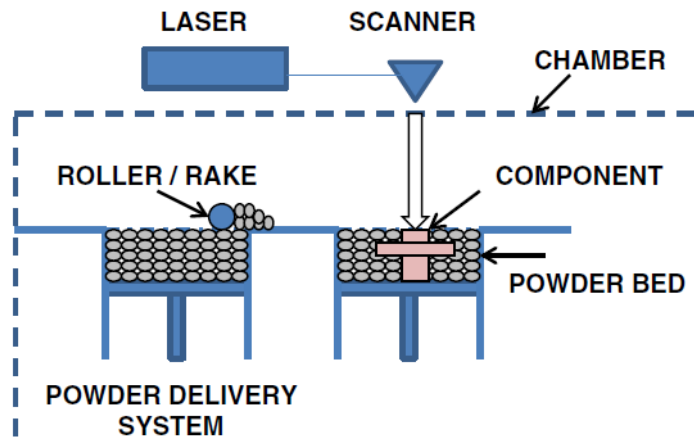


Figure 2.5 Generic illustration of a powder bed feed system [2].

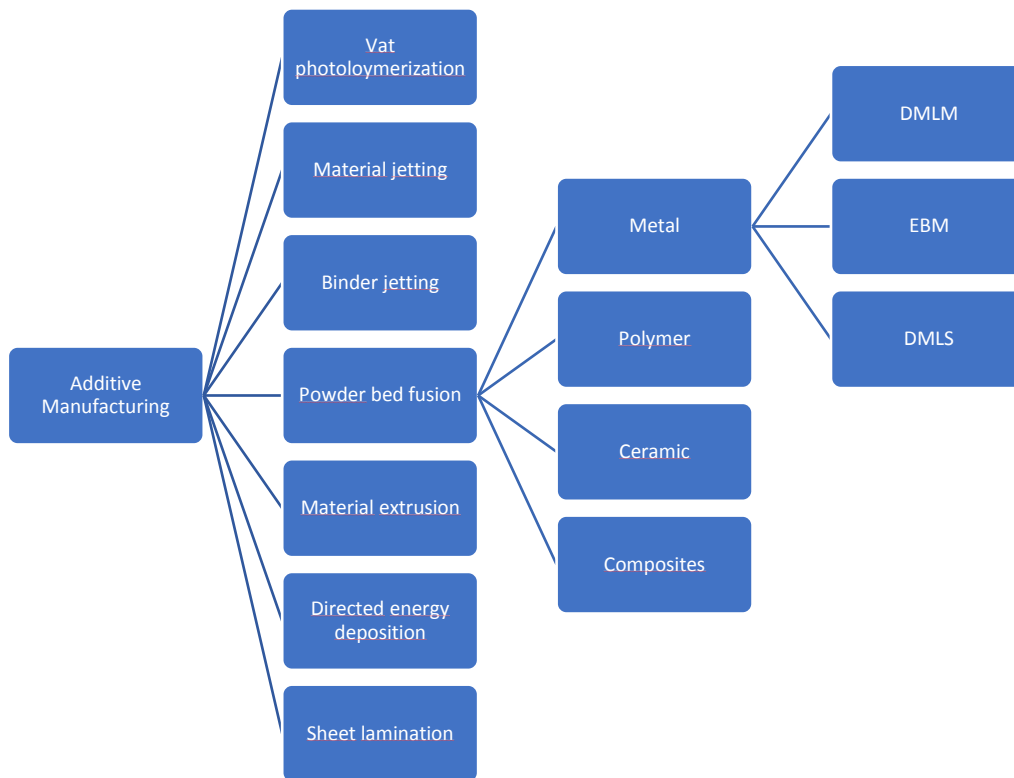


Figure 2.6 Localization of the technologies for powder bed fusion metal additive manufacturing.

- Electron Beam Melting (EBM)

In the EBM system, electrons are generated in a gun and accelerated with a certain difference of potential, focused using electromagnetic lenses and electromagnetically scanned. Consequently, beam deflection is achieved with no moving parts. The focused electron beam is initially scanned with a high beam current to preheat the powder for a better conductivity, then the final melt scan produces melt pools or zones related to the beam diameter and scan spacing. This good thermal environment leads to good form stability and low residual stress in the part. Mean or average powder particle sizes can range from 10 μm to 60 μm . Like any electron beam system, the EBM system operates under a vacuum of 10^{-4} atm [6], which is beneficial when it comes to work with reactive alloys, e.g. titanium.

The introduction of General Electric in this market produced in 2017, when the Swedish company Arcam AB joined the business unit of GE Additive incorporating all its product portfolio of machines and powder generation. For instance, their newest launch is the Spectra H model, which has a build plate of 250 mm diameter x 430 mm height and a better control in powder quality and insulation.



Figure 2.7 Spectra H machine from Arcam, the newest machine in the EBM field [7].

- Direct Metal Laser Melting (DMLM)

The DMLM utilizes a focused laser beam to create the melt pools. The average diameter of the laser beam is typically of 100 μm , and it is scanned by a CAD driven rotating mirror system and focused into the powder bed. A mechanical recoater similar to the raking system in the EBM forms the powder layers onto the build platform. Powder is fed from a supply container while excess powder is collected for recycle.

During the DMLM process, the build platform is heated to 90 $^{\circ}\text{C}$, considerably cooler than the EBM build environment. The laser beam scans in the XY plane to form melt pool arrays similar to EBM melt scanning. In the DMLM, the EBM vacuum system is replaced by either purified argon or nitrogen, which in addition to providing oxidation protection by purging the oxygen from the system, provides efficient heat conduction and component cooling.



Figure 2.8 Concept Laser XLine 2000R [8].

The mechanical properties of metals processed by DMLM exceed those of investment casting and almost reach those of wrought materials.

Like in the previous case, General Electric has put the spotlight in this technology by joining the German company Concept Laser in 2016 to their GE Additive division, not only offering their production machines portfolio, but further development and transformation of the industrial sector with software-defined plants. One of the examples of the multiple machines that Concept Laser offers is the XLine 2000 R, with a building envelope of 800 x 400 x 500 mm³.

- Direct Metal Laser Sintering (DMLS)

Like the DMLM, the DMLS uses a laser beam as the energy source. The difference between processes is the physical union that is established. In sintering, with the correct combination of temperature and pressure, the powder particles will tend to reduce their free energy by reducing their surface area, thus packing closely getting the fusion of the particles, but without arriving to the melted state. This occurs at temperatures between one half of the absolute melting temperature and the melting temperature. As the particles do not experiment a phase change, there might be some areas in where the melting is not achieved, producing undesirable porosity. This parameter is time-controlled, i.e. the more time the energy source is applied the less porosity; or temperature controlled, i.e. the more sintering temperature the less porosity as well.

2.2. Applications

The fields where the most promising applications for additive manufacturing can be found are:

- Aerospace: lightweight, high temperature (cooling and heat exchanging), complex geometry (components with multiple functionalities), economics (low production volumes), digital spare parts (instead of warehousing spares and tools to have a digital library of spares to build on demand).
- Medical: prosthetics, diagnostics and surgical aids, tissue engineering.
- Automotive: nowadays only applicable in businesses with low volume production, rapid prototyping to detect problems in operations in assembly lines, formula 1.

Normally a 1 to 1 substitution is not a win for additive manufacturing. The challenge for a designer is to identify parts and assemblies where using the freedom to design creates an added value and by this justifying the additional costs of additive manufacturing. Therefore, it is needed to find the

potential benefits of a parts combination, or functionalities combination, or elimination of downstream post-process operations for detailed features.

2.3. Generic AM process

According to [3], the process of building a part by means of AM can be divided into the next steps:

1) CAD

The 3D CAD model is sliced into layers and transferred to the machine.

2) Conversion to STL format

STL (Stereolithography) format uses triangles to describe the external closed surfaces of the original CAD model to be built and forms the basis for calculation of the slices. Each triangle is described as three points and a facet normal vector indicating the outward side of the triangle, in a manner like the following:

```
facet normal -4.470293E-02 7.003503E-01 -7.123981E-01
outer loop
vertex -2.812284E+00 2.298693E+01 0.000000E+00
vertex -2.812284E+00 2.296699E+01 -1.960784E-02
vertex -3.124760E+00 2.296699E+01 0.000000E+00
endloop
endfacet
```

Figure 2.9 STL format template to define a single triangle.

Nearly every AM machine accepts the STL file format, which has become a standard, and nearly every CAD system can output such a file format. The STL file format was made public domain to allow all CAD vendors to access it easily and integrate it into their systems.

3) Transfer to the machine

Adaptation of the STL file to the machine environment, to ensure optimal size position and orientation of the part or to optimize the use of all the printing chamber surface to reduce waste. For instance, in this step auxiliary supports can be designed to relieve thermal residual stress or to guarantee good manufacturability in downfacing surfaces.

4) Machine setup

Before launching the build job, several parameters must be set in order to fit the characteristics of the machine with the needs of the component to achieve the best combination of production parameters such as build time, laser diameter, material specific characteristics or layer thickness.

5) Build

Building the part is mainly an automated process and the machine can largely carry on without supervision. Only superficial monitoring of the machine needs to take place at this stage to ensure no errors have taken place like running out of material, power or software glitches, etc.

6) Removal and cleanup

In some cases, depending on the method applied, it is necessary to remove the part from the building plate with the consequent interaction with the machine.

The quality of the part right after being printed may not be the desired. To improve it, some manipulations must be done to increase the density material, relax thermal stresses or remove auxiliary support structures from the body of the part. Treatments may be laborious and lengthy if the finishing requirements are very demanding.



Figure 2.10 Pre- and post-processed part printed with AM.

7) Post processing

This step refers to the stages of finishing the parts for application purposes. This may involve abrasive finishing, like polishing, or application of coatings. The amount of cycle time spent at this stage can be very variable, as every AM part is designed differently and post process becomes usually a manual task due to complexity. However, some of the tasks can benefit from the use of power tools, such as CNC milling.

8) Application

The part is ready to be assembled and to develop its functions.

2.4. Manufacturing guidelines for metal AM

Not all parts of a system are equally suited for Additive Manufacturing or bear the same potential for an improvement of the overall system. An analysis of the predecessor or an initial design identifies those parts where a change in manufacturing technology provides the biggest benefit to the system's performance. For instance, in [9] a criterium to identify potential improvements is presented to assess the suitability of this technology for design.

Some of the limitations that one can find while designing for manufacturing can be found below. The values reported can vary from one technology to another, but in every case, can be considered as characteristic manufacturing limitations.

- Wall thickness

From the literature ([10], [11]), an illustrative value for the minimum wall thickness manufacturable with AM can be considered ca. 1 mm. Naturally, this value can be pushed to lower thickness if the material and the technology allows it. Another parameter to consider in this case is the efficient transport of heat during the printing, i.e. the presence of support will help to build thinner thicknesses.

- Build rate

The orientation of parts is a key driver for printing efficiency, especially the effect of the height of the part in the building direction. As the recoating time does not add any material and therefore any value to the printed part, it is recommendable to orient the part such a way that each melting time will be optimized. Thus, the height has to be the minimum as possible to try to print the body using the less number of layers to avoid these recoating times.

- Lateral holes

Lateral holes that emerge on the side faces of parts may also require supports. The minimum size of hole that it is sensible to build on most laser powder-bed machines is 0.4 mm.

Holes and tubes larger than 10 mm in diameter will require supports in their center, and should be considered for re-design. Holes below these dimensions may be produced without supports, but are likely to suffer from some distortion on their down-skin surfaces due to slow cooling of the weld pool above the overhang.



Figure 2.11 Effect of diameter in lateral holes.

Since lateral holes are unlikely to be perfectly round, it often makes sense to change their shape so that they are self-supporting. In some cases, a teardrop or diamond shape may be acceptable for the finished feature. In other cases, where a precision, round hole is essential, then post-process machining will be needed. In fact, in many cases filling the hole and machining it from solid can make the most sense.

- Part orientation

In powder-based processes, where shapes are built up layer by layer, the way these layers relate to each other is important. As each layer is melted, it relies on the layer below to provide both physical support and a path to conduct away heat.

When the laser is melting powder in an area where the layer below is solid metal, then heat flows from the weld pool down into the structure below, partially re-melting it and creating a strong weld. The weld pool will also solidify quickly once the laser source is removed as the heat is conducted away effectively.

Where component features overhang those below, then at least part of the zone below the weld pool will consist of un-melted powder. This powder is far less thermally conductive than solid metal, and so heat from the melt pool is retained for longer, resulting in more sintering of surrounding powder. The result can be additional material attached to the bottom surface of the overhanging region, meaning that overhangs can exhibit both misshapen surfaces and a rough

finish with undesired powder attached. In fact, the resulting structure after the printing is called the cake due to the appearance given by the partially sintered powder.

- Resolution and surface finish

Since additive technology builds objects in layers, there is inevitably a staircasing effect produced by the discretization of CAD surfaces. Moreover, thermal warping is one of the drivers for a successful printed job. The residual stresses are a result of the local melting and non-uniform cooling of the part during manufacturing. In fact, this is one of the reasons for the use of supports to evacuate the heat flow generated by the melted section.

The finish and appearance of a part are related to accuracy, but also depend on the method of RP employed. Technologies based on powders have a sandy or diffuse appearance, sheet-based methods might be considered poorer in finish because the staircase is more pronounced.

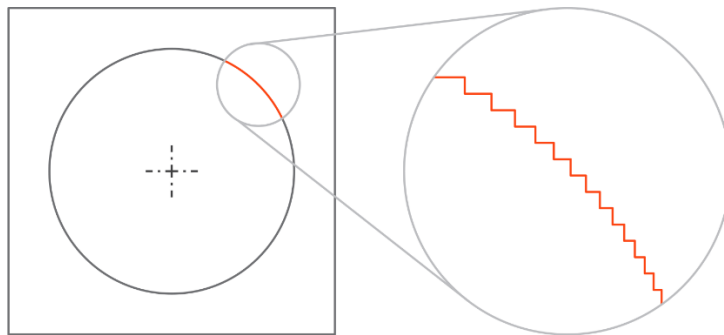


Figure 2.12 Staircase effect.

- Orientation of features

The orientation of the part with respect to the recoater rake is important, as during the deposition of a new powder layer the recoater may interact with surfaces inclined towards the wiper, squeezing them risking the structural integrity of the part and leading to a failed build. Supports and inclined edges should therefore be orientated away from the wiper direction where possible. By tilting the part a small angle (around 5°), the pressure wave now strikes the part at an oblique angle, reducing the likelihood of distortion.

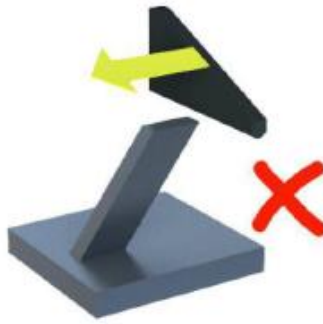


Figure 2.13 Orientation of the part with respect to the recoater is important.

- Residual stress

Residual stress is a natural consequence of the rapid heating and cooling. Heat flows from a hot melt pool down into the solid metal below and so the molten metal cools and solidifies this all happens very rapidly in a matter of microseconds. As layers are added on top of one another the residual stresses build up, and can lead to a distortion of the part and even the failure of the build if the stress exceeds the strength limit of the building material.

The scanning often occurs in two modes, contour mode and fill mode. In contour mode, the outline of the part cross section for a particular section for a particular layer is scanned. This is typically done for accuracy and surface reasons around the perimeter. In some cases, the fill section is subdivided into strips (where each strip is scanned sequentially and the strip angle is rotated every layer) or squares (with each square being processed separately and randomly). Randomized scanning is sometimes utilized so that there is no preferential direction for residual stresses induced by the scanning. Typical direction change between layers is 67°.

Post process treatments can relieve residual stresses as well as the heating of the build plate, such as Hot Isostatic Pressure (HIP) and shoot peening.

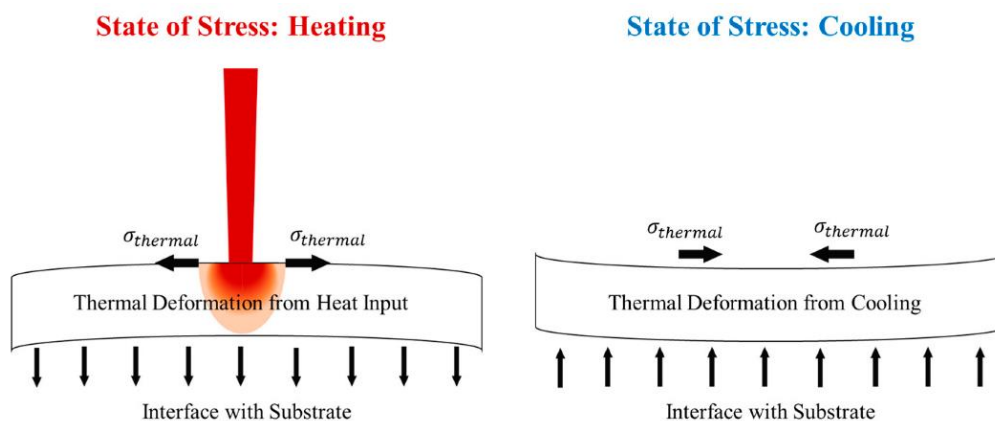


Figure 2.14 Residual stress after melting the powder layer [12].

3. Structural optimization methods

As structural optimization methods, finite element analyses are performed typically during each iteration of the optimization method, which means that all the methods presented below can be computationally time demanding. Consequently, structures obtained by this kind of methods will make use of the minimum and essential material to achieve the imposed objective and constraints

Here the purpose is to find the optimal material distribution according to some given boundary conditions of a structure. Some common functions to minimize are the mass, displacement or the compliance (strain energy). This problem is most often subject to some constraints on the mass or on the size of the component. The formulation of the problem of optimization could be described as follows. Find

$$\mathbf{x} = \begin{Bmatrix} x_1 \\ \vdots \\ x_n \end{Bmatrix} \quad (3.1)$$

Which minimizes $f(\mathbf{x})$ and subject to:

$$\begin{cases} g_i(\mathbf{x}) \leq 0, & i = 1, 2, \dots, m \\ h_j(\mathbf{x}) = 0, & j = 1, 2, \dots, n \end{cases} \quad (3.2)$$

Where \mathbf{x} is the vector of design parameters and $f(\mathbf{x})$ is the function to minimize. The functions $g_i(\mathbf{x})$ and $h_j(\mathbf{x})$ define the constraints of the problem. This is called a constrained optimization problem.

It must be remarked that modern numerical techniques of structural optimization were already conceived and developed many years before AM made its appearance in the manufacturing industry it has been now that all the benefits of these techniques start to be attractive from an industrial point of view thanks to the fact that AM is a technology that allows to build all the geometries generated by the algorithms. The list below reports some of these techniques for the general knowledge underlining their main characteristics.

3.1. Topology optimization

The most general form of structural optimization is topology optimization. The purpose is to find the optimum distribution of material. From a given design domain the purpose is to find the optimum distribution of material and voids, while all the constraints and boundary conditions are satisfied. To do so, the volume domain is divided into design and non-design space. In the first one the algorithm lets the normalized density take any value between zero and one while in the latter

the material density will be equal to one, i.e. full, to ensure design considerations and/or requirements.

For a typical design problem, engineers work under the restrictions that the component must be able to withstand certain loads, and that its layout cannot extend beyond the limits of the design space.

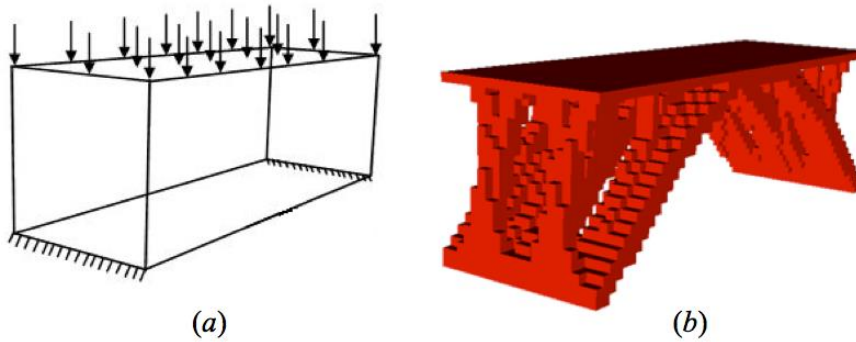


Figure 3.1 Topology optimization.

The software package OptiStruct [13] solves topological optimization problems using either the homogenization or density method. Under topology optimization, the normalized density of each element should take a discrete value of either 0 or 1, defining the element as being either void or solid, respectively.

3.1.1. SIMP method

The density-based TO method, proposed decades ago by [14] is most common, and is used in the commercial software packages, is known as the SIMP (Solid Isotropic Material with Penalization) method. A density value of 1 indicates that the material is fully dense, while a value of 0 indicates that no material is present.

As it is not desirable, Young modulus of the material with intermediate densities is penalized so that the density of the material will tend to be full or empty at the end of the optimization. The stiffness of the material is assumed to be linearly dependent on the density. The following correlation of the elastic property with density is applied:

$$E(x) = \rho(x)^p E_0 \quad (3.3)$$

The equation (2.3) is presented in fig.3.2 where:

- x is the position vector inside the design domain;
- ρ is the relative density at the position x ;

- $E(x)$ is the material stiffness at the position x ;
- p is the penalty factor.

the penalization exponent typically takes a value between 2 and 4 depending on the aggressiveness of the optimization. As a rule of thumb, the default value of the penalization factor is 1 for shell dominant structures and 2 for solid dominant structures with member size control (i.e. minimum dimension of the resulting optimized elements). For non-solid dominant models, when minimum size control is used, the penalty starts at 2 and is increased to 3 for the second and third iterative phases.

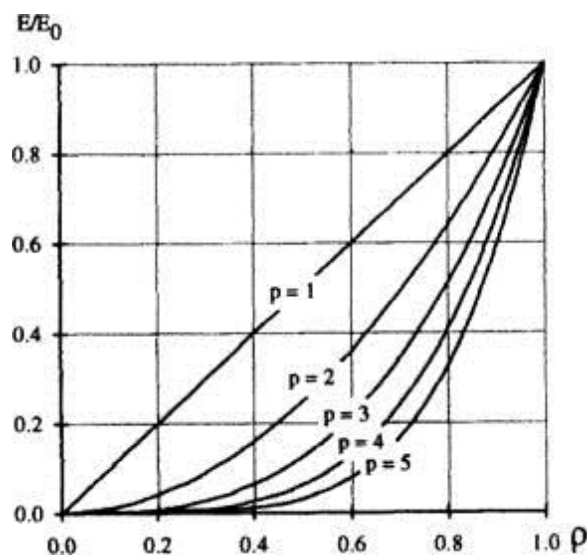


Figure 3.2 effect on the density value for different values of the penalization parameter.

The influence of the parameter p is crucial for the result of the optimization. Thus, as the penalty factor increases then the solution is more discrete and material and voids are more defined, but it is more probable to have checkerboard problem, i.e. the generation of geometries composed by an alternation of full and void elements avoiding a well-defined geometry. These discontinuities in the transition of the density provoke the presence of isolated elements or not well joined structures, making the solution concept unfeasible,

3.2. Lattice optimization

The extensive use of additive manufacturing and the forecasted demand of the growth of the market share has brought the focus to the possible developments that can make additive even more attractive as the process choice. Lately, many technical software companies have brought the spotlight into the development optimization solvers that exploits one of the main advantages of additive manufacturing: the lattice structures.

The lattice structures are one step forward for the creation of lighter and more efficient structures from the point of view of stiffness and thermal that additive has made possible due to the slicing of the part in sections.

From the point of view of the optimization algorithm, lattice optimization can be divided into two phases:

- First phase: classical topology optimization, letting porous zones in the material to appear by loosening the penalization process. A control in the porosity of the material can be done by penalizing the structural properties as well (i.e. Young modulus) of the porous material.
- Second phase: Conversion of the porous resulting design space into lattice elements with different cell geometries defined by the user. Each cell element is formed by junctions of beam elements. The scope of this phase is to optimize every beam diameter of every lattice structure to achieve the optimal performance with the minimum quantity of material. Hence, not only the distribution of lattice has been achieved, but also the optimization of every single sub element, making this technique very promising, despite a lot of work has still to be done as this is a very new technique.

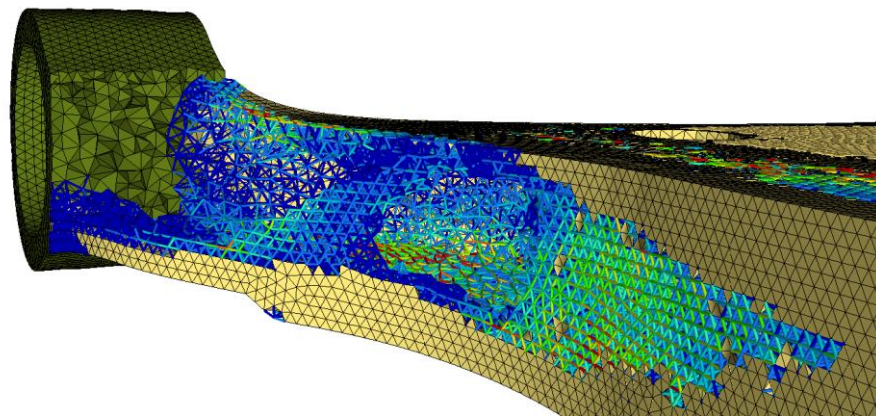


Figure 3.3 Lattice optimization example where the load distribution between lattice elements is optimized [13]

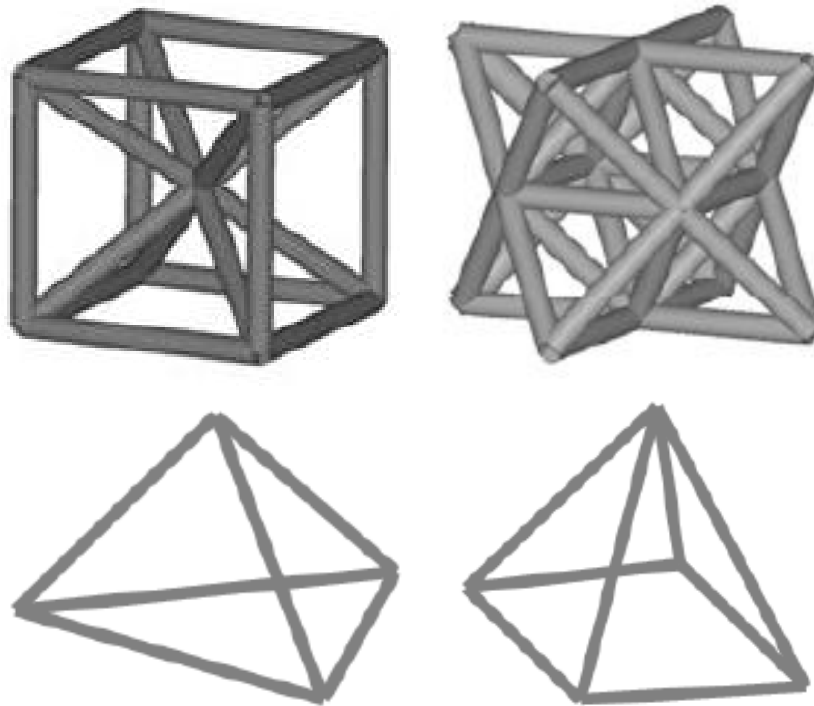


Figure 3.4 Examples of different type of lattices available depending on the type of solid element replaced [13].

3.3. Size optimization

In size optimization, the properties of structural elements such as shell thickness, beam cross-sectional properties, spring stiffness and mass are modified to solve the optimization problem.

In finite elements, the behavior of structural elements such as shells, beams, springs and concentrated masses are defined by input parameters such as shell thickness, cross sectional properties and stiffness. Those parameters are modified in a size optimization.

3.4. Free-size optimization

Is a mathematical technique that produces an optimized thickness distribution per element for a 2D structure (i.e. shell elements). For a shell cross-section, free-size optimization allows thickness to vary freely between T and T_0 for each element; this contrasts with topology optimization which targets a discrete thickness of either T or T_0 .



Figure 3.5 Range of the values that thickness can adopt in the free-size optimization.

The motivation for the introduction of free-size is based on the conviction that limitations due to 2D modeling should not become a barrier for optimization formulation.

It is important to note that while the free-size design concept generally achieves better performance when buckling constraints are ignored, the topology concept could outperform free-size, if buckling constraints become the driving criteria during the size and/or shape optimization stage. The reason for this is that topology optimization eliminates intermediate thicknesses, which leads to a more concentrated material distribution and a shell that is stronger against out-of-plane buckling.

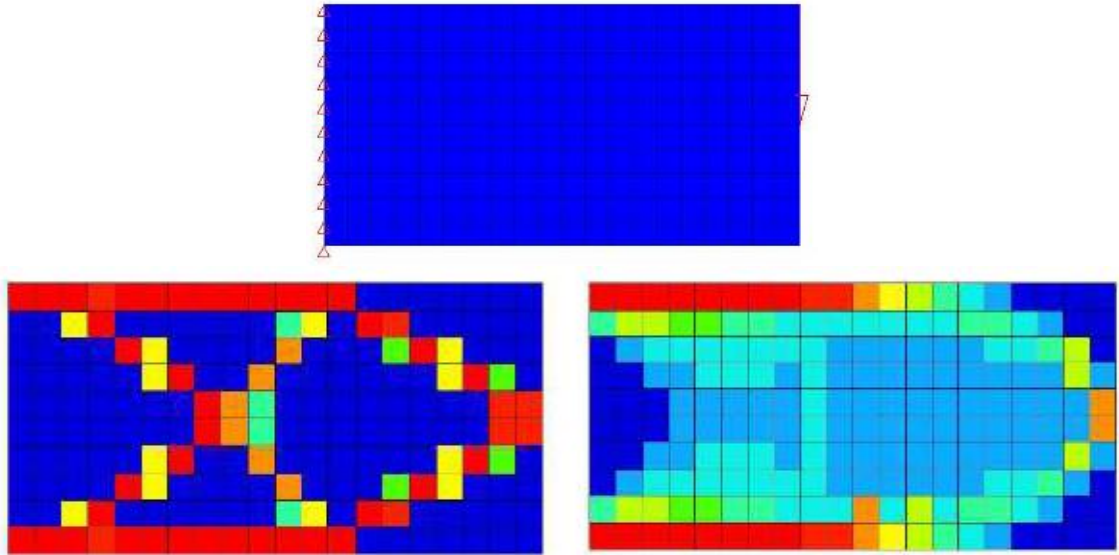


Figure 3.6 Free-size optimization.

3.5. Shape optimization

A parametric shape is defined by a finite, and usually small set of geometric parameters called dimensions, e.g. radii. Parametric shape optimization searches the space spanned by the design variables to minimize or maximize some externally defined objective function, normally one of the above mentioned geometric parameters.

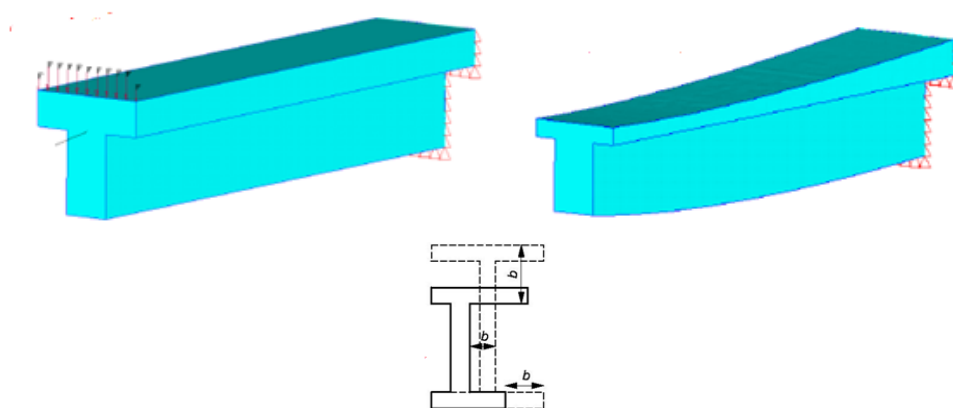


Figure 3.7 Shape optimization.

Is an automated way to modify the structure shape based on predefined shape variables to find the optimal shape. In shape optimization, the outer boundary of the structure is modified to solve the optimization problem. Using finite element models, the shape is defined by the grid point locations. Hence, shape modifications change those locations.

3.6. Topographic optimization

Is an advanced form of shape optimization in which a design region for a given part is defined and a pattern of shape variable-based reinforcements within a region is generated using OptiStruct.

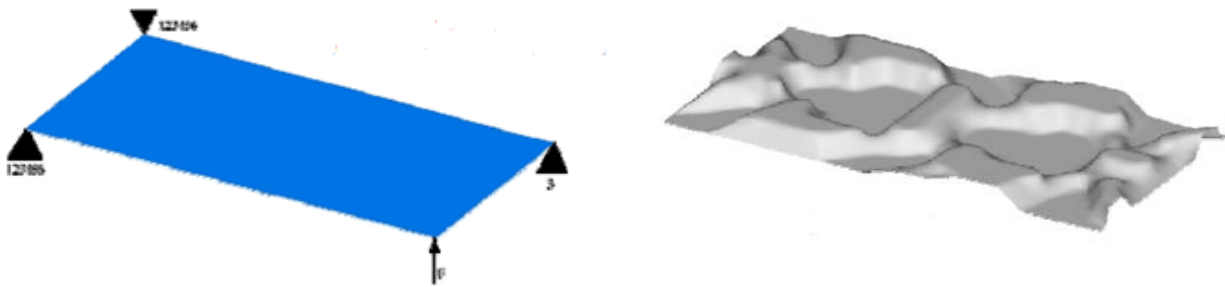


Figure 3.8 Topographic optimization.

The approach in topography optimization is similar to the approach used in topology optimization, except that the shape variables are used rather than density variables. The design region is subdivided into a large number of separate variables whose influence on the structure is calculated and optimized over a series of iterations. The large number of shape variables allows the user to create any reinforcement pattern within the design domain instead of being restricted to a few.

3.7. Free-shape optimization

Is an automated way to modify the structure shape based on set of nodes that can move totally free on the boundary to find the optimal shape to meet with the pre-defined objectives and constraints. Where it defers from other shape optimization techniques is that the allowable movement of the outer boundary is automatically determined, thus relieving users of the burden of defining shape perturbations. Free-shape optimization allows these design grids to move in one of two ways:

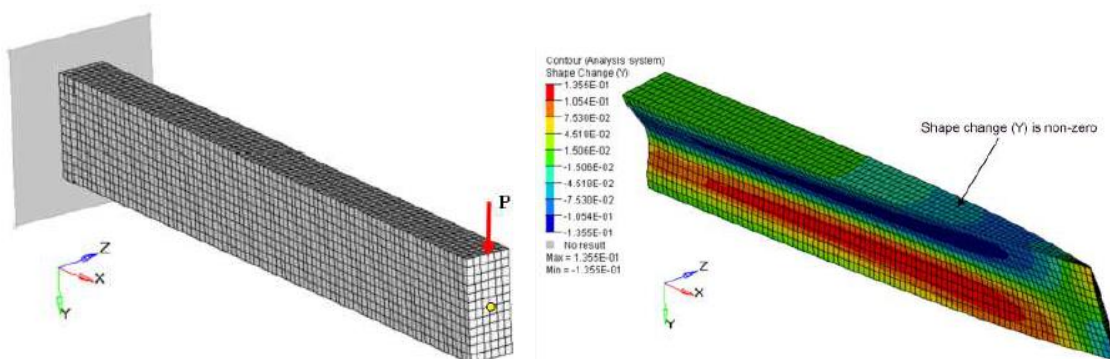


Figure 3.9 Free shape optimization of a clamped beam. The design regions are the vertical outer surfaces of the beam.

- For shell structures, grids move normal to the surface edge in the tangential plane.
- For solid structures, grids move normal to the surface.

4. Problem definition: Pitch Control Unit (PCU)

The case study of this thesis is focused in a system belonging to a turboprop, where most of the power generated in the turbine is transmitted to a propeller through a reduction gearbox. The rest of the power generated is to drive the compressor or exhausted in the propelling nozzle to add a small amount of thrust to the engine.

4.1. Description of the system

The propeller is driven by the power turbine through the propeller gearbox (PGB). The PGB decreases the power turbine's rpm to a speed compatible with propeller operation.

The objective of the system is to modulate propeller pitch such that smooth thrust control is achieved in a manner that is safe, reliable and efficient. This is possible with a Pitch Control Unit (PCU), whose purpose is to control the flow of hydraulic oil in response to the signals from the electronic controller.

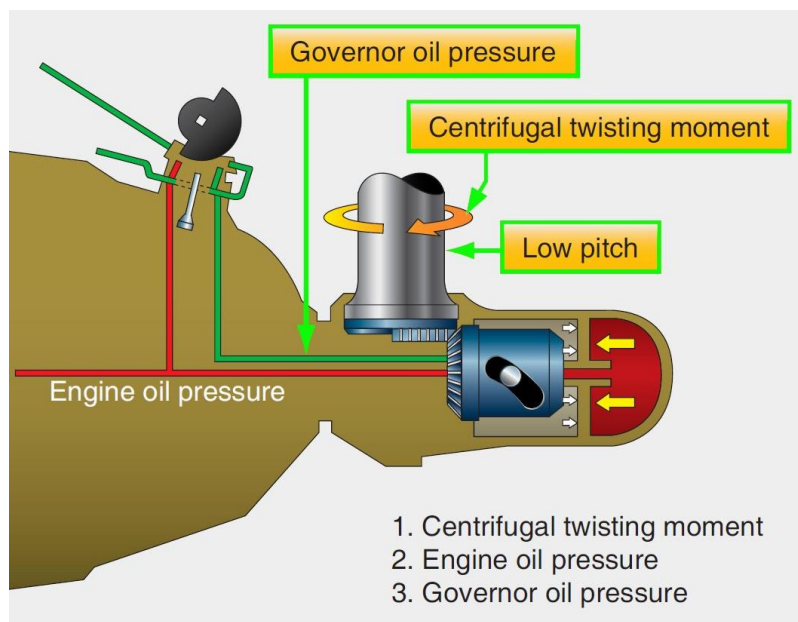


Figure 4.1 Propeller mechanism to get a pitch variation from the beta tube [15].

Blade pitch change is achieved by regulating the flow and pressure of oil inside the pitch change piston through the beta transfer tube. The linear motion of the piston is translated into blade rotation through the operating pin/crosshead arrangement. A governor controls blade angle for constant-speed propeller operation. In the event of a failure of the propeller actuator, the propeller counterweights placed in the root of the blades are sized and phased to provide sufficient centrifugal effort to drive the propeller towards a safe operation pitch.

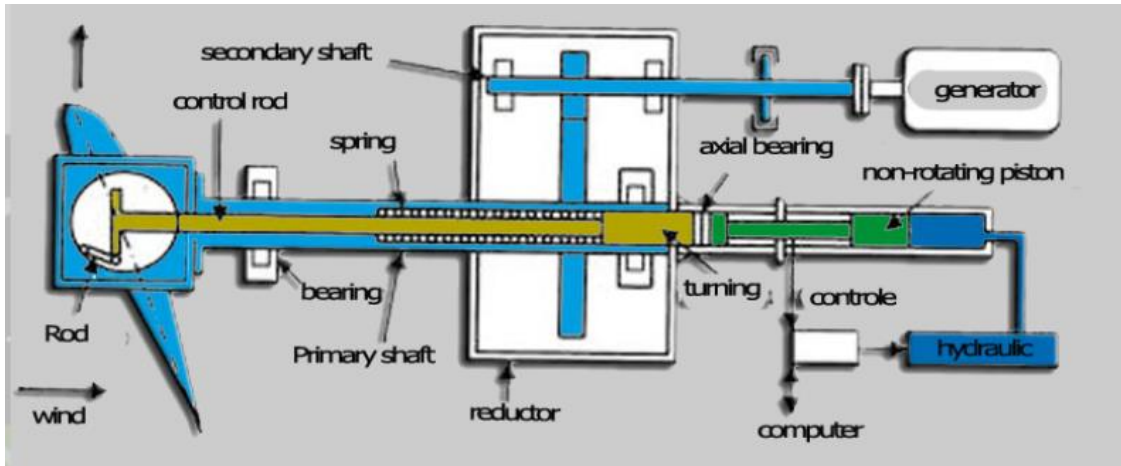


Figure 4.2 Operating scheme of a generic PCU [16].

The schematized assembly of the PCU is showed in fig. 4.3 showing the volume envelope of the PCU, which is intended to be reduced in order to help for assembly. Due to confidentiality reasons for the sensitivity of the information of the real PCU, the assembly has had to be schematized to show the baseline's shape.

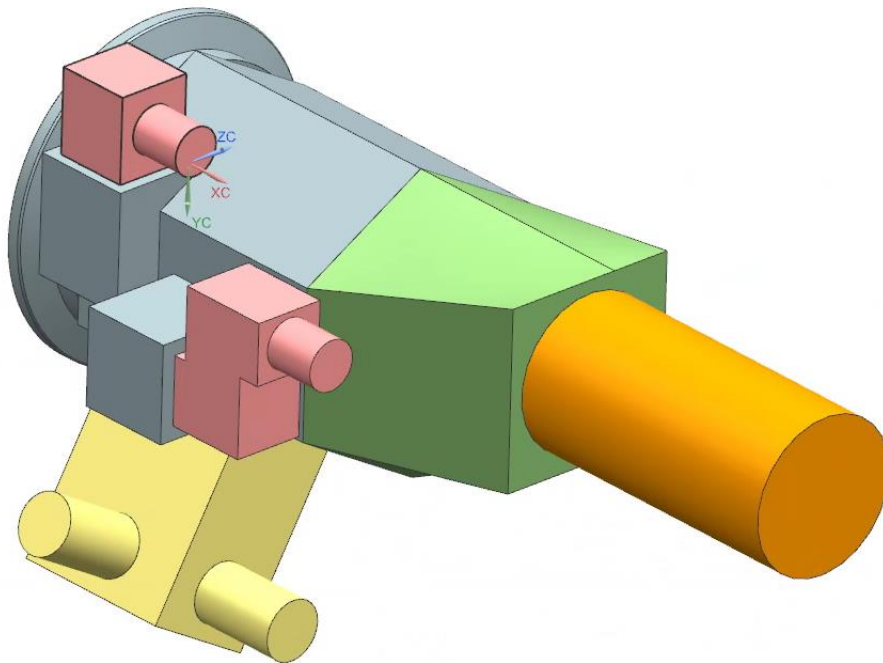


Figure 4.3 Scheme of the assembly of the PCU.

The main pressure supplies to this unit are three pump sources: high pressure pump (HPP), the overspeed governor (OSG) and the feathering pump. The first two provide pressure directly from the Propeller Gearbox of the engine (PGB) while the feathering pump is an independent gear pump to provide pressure mainly for maintenance purposes.

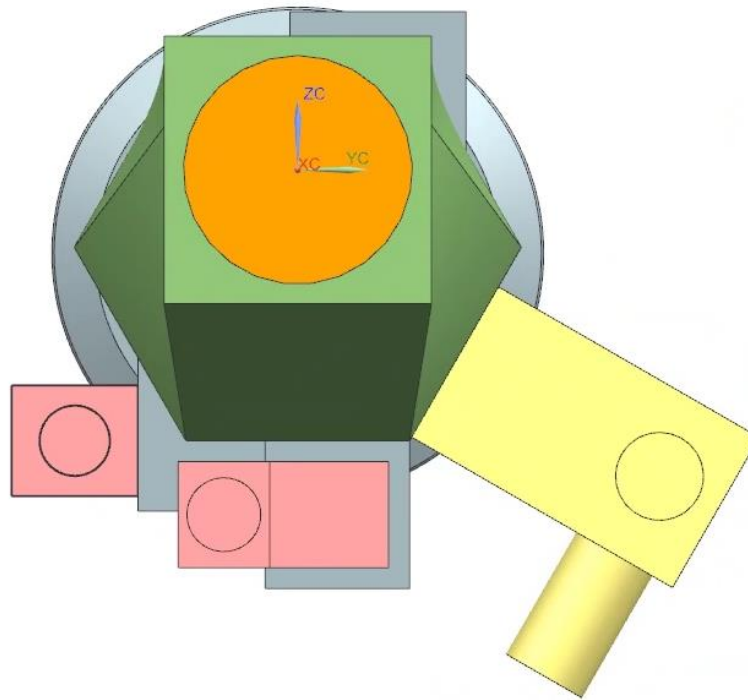


Figure 4.4 Rear view of the assembly.

Fig. 4.4 serves to introduce one of the main potential improvements in the redesign: the original position of the pink connectors is not adequate from the point of view of engine integration, i.e. they were positioned too downwards in the bottom of the unit. The reason to state this is that there were other surrounding elements that caused an undesirable interference when the PCU was fitted in the engine. This issue was identified as an important point to take into account, especially when the connectors are supposed to be parts of the unit provided with an ergonomic access as they have to be plugged and unplugged frequently by the maintenance technicians.

4.1.1. Assembly components

- Main body

The main body contains all the hydraulic elements to control the PCU. The spool valves are assembled in the inside of the body and the external part contains the interfaces to assemble the electrical connectors for the solenoid and the servo valve. Furthermore, all the connections between valves necessary for the operation are contained inside the body. In conclusion, the main body is a vital element for the PCU as it gathers many of the functions of the system. Nevertheless, its geometrical complexity and the accumulation of functions in such a reduced space makes this component very bulky and heavy when the conventional subtractive manufacturing technologies are applied, while the variety of tooling needed to perform all the featuring operations is very broad. In short, this component was identified as the perfect candidate to redesign for additive, and

therefore is going to be from now on the subject for the topological optimization. One of the main reasons for this decision was the potential mass saving that can be achieved using additive, maintaining the complexity and at the same time its operating functionalities.

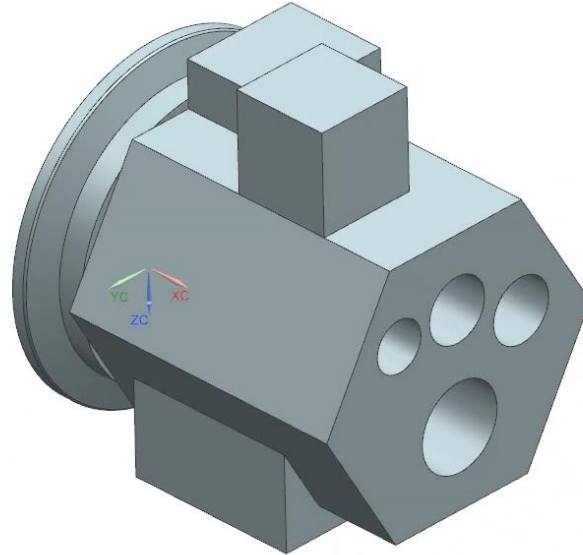


Figure 4.5 Main body of the PCU schematized.

- Mid-housing

The mid-housing acts as an interface between the main body and the transducer. Its geometry adapts to the mating interfaces to serve as the transition between components. At the same time, it has to provide sealing resistance as the inner part when assembled contains all the oil drained from the valves. To ensure this, a tailored gasket with the profile of the mating interface is mounted between the main body and the mid-housing.

- Beta Feedback Transducer

The Beta Feedback Transducer (BFT) is the element that monitors the axial position of the beta tube. This is an implicit method to monitor the blade pitch angle, as both magnitudes are mechanically related. The overall length of the BFT is determined by the envelope of axial positions of the beta tube. Indeed, independently of the operating regime of the propeller, the beta tube needs space availability to move back and forth to set the pitch angle properly. Through this component the flight computer receives the feedback of the angle to achieve a closed loop control.

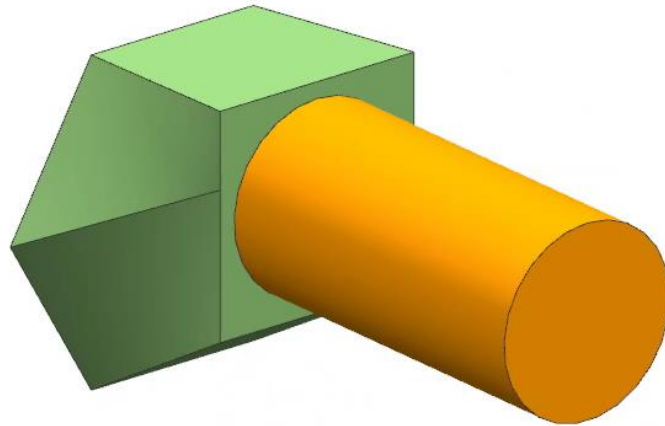


Figure 4.6 Mid-housing (green) and Beta feedback transducer (orange) schematized.

- Electrical connectors

The electrical connectors are showed as the colored parts attached to the main body in the fig. 4.7. Their function is to transmit the electric commands from the flight computer to the valves. From the design point of view, the interfaces of assembly must be conserved as the connectors are not object of the redesign. However, the position of these interfaces can be moved freely.

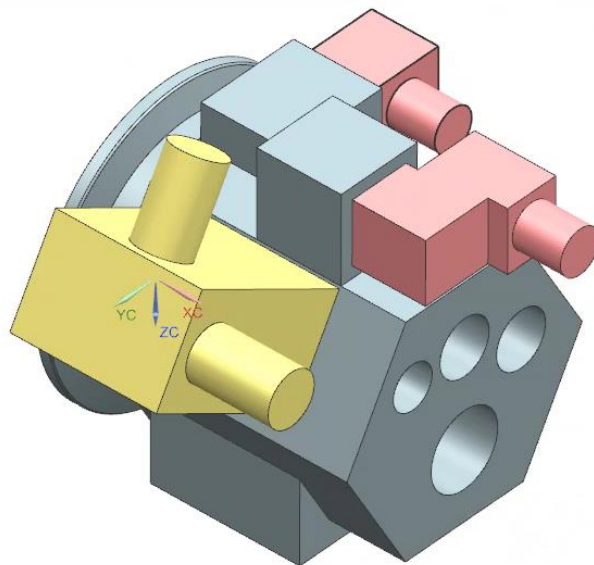


Figure 4.7 Schematized electrical connectors of the valves. All of them are bolted to the main body.

4.1.2. Hydraulic valves

To control the flow of hydraulic liquid at every operation regime, different types of valves are used in the PCU, which are: solenoid, spool, non-return and servo valves. A brief description of each of them is made below to understand the operation principles and the typical geometries that can be found.

- Solenoid:

This kind of valves is controlled by an electric current through a solenoid. Depending on the electric current, the solenoid is energized creating an electromagnetic induced force. They are the most frequently used control elements in fluidics. Their tasks are to shut off, dose, distribute or mix fluids. In the case study of this work the solenoid valves have the mission of switch on or off the flow.

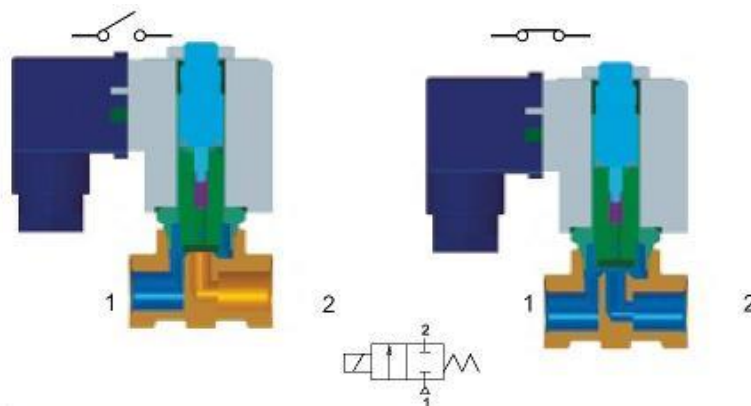


Figure 4.8 Scheme of a solenoid valve.

When the electric signal arrives from the controller, the spool moves due to the force above mentioned changing the passage of oil.

- Spool:

These valves are controlled in such a way that the spool moves back and forth inside the sealing sleeve into different positions, connecting pressurized ports or draining liquid to the sump depending on the operation requirements. The control in the case of the PCU was made by a spring, which controlled the amount of displacement of the spool depending on the source of pressure.

By actuating this valve, the spool shifts, opening the ports to allow for oil flow. One thing to bear in mind for this type of valves is that the sleeve and the spool must be made of the same material, otherwise a difference in thermal expansion coefficients can cause greater leakage and even jamming of the spool, risking the operation of the unit.

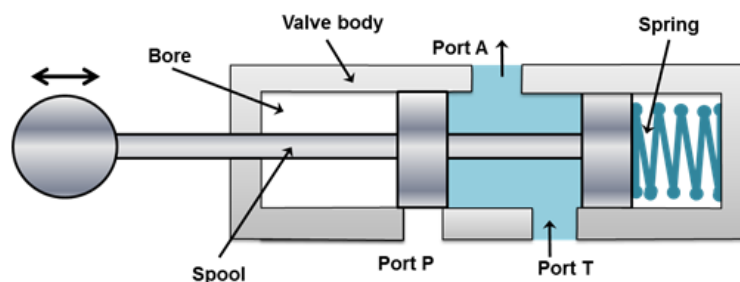


Figure 4.9 Scheme of a spool valve.

- Servo:

A more sophisticated application of the spool valves can be found in the case of the servo valve. The basic working principle is the same, with a spool valve controlling the oil flows. However, servo valves incorporate a closed-loop control thanks to a mechanical spool position feedback which provides for flow or pressure outputs that are proportional to the electrical input. As a result, a faster and more accurate control of flow is obtained, allowing even the possibility of quick reversal of flow if the computer schedules a change in the regime of operation.



Figure 4.10 Operation scheme of a servo valve.

- Non-return:

Non-return valves, also known as check valves, allow the liquid to flow only in one direction, stopping the flow in the case the liquid would try to invert the flow direction.

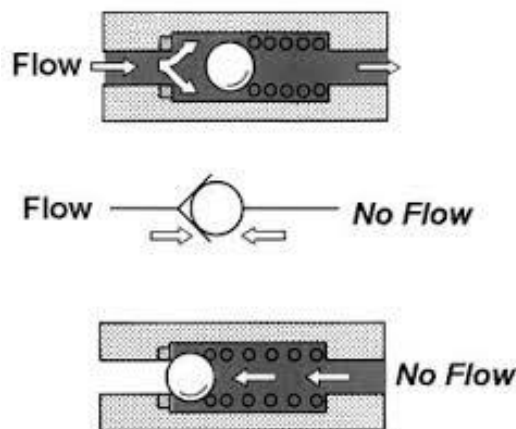


Figure 4.11 Scheme of a non-return valve.

They are a very common element in hydraulic systems because they are simple, autonomously controlled and small. In the case of this study case the bore where the valve is installed needs to be necessarily drilled and successively plugged, avoiding a possible integration of parts and maintaining one post process operation after the additive printing.

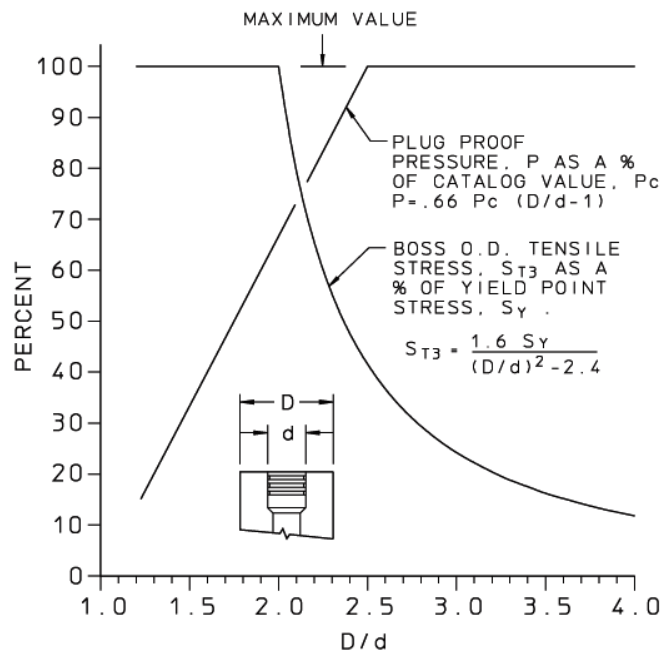


Figure 4.12 The effect of D/d ratio on stresses for plug and boss material with similar mechanical properties. [17]

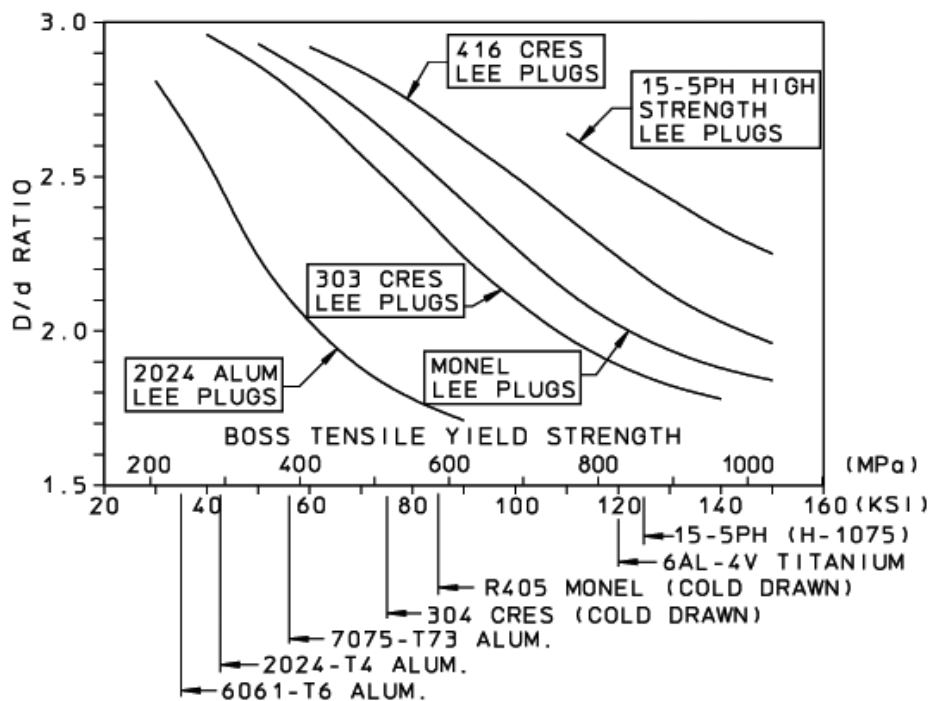


Figure 4.13 Effect of D/d ratio on plug and boss dissimilar mechanical properties. [17]

Additionally, one requirement for the assembly of the plug of this valve concerns the minimum diameter of surrounding material around the hole to plug properly the plug. This is necessary to

ensure stress concentration resistance during the assembly of the plug, which is normally pushed into the hole and deformed to fit the possible voids and guaranteeing sealing. After consulting the supplier data and considering a conservative approach, it was obtained that the minimum diameter of material surrounding the hole had to be 2.8 times greater than the diameter of the hole itself.

5. Design optimization

Once the original PCU has been presented, the redesign process is ready to be set up to identify potential improvements to make to the original design relying on additive technology. Firstly, the most constraining identified design driver in this case was the position and the form of the beta transfer tube, as its axiality with the beta tube is crucial for the operation of the system. Secondly, it was decided to maintain or increase the values of all the cross-sections areas for the internal channels to ensure the necessary flow of hydraulic oil in every operation condition. Thirdly, the external shape of the resulting concept was free to choose except for the interfaces with the electric connectors.

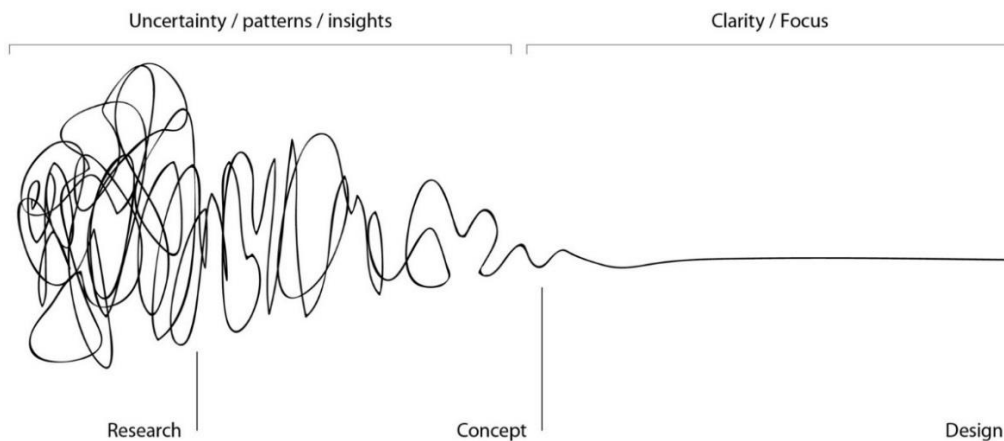


Figure 5.1 The design process simplified.

Therefore, all the elements were subject to changes in the position making possible a more compact option in which the engine integration was considered as well.

5.1. CAD modeling

Different layouts for the valves were considered in the conceptual initial design to find an optimum configuration both in terms of compactness and engine integration and at the same time respecting all the internal functionalities. As a result, a wide number of conceptual schematic layouts were developed to harness the fact that this is a design from scratch and therefore the design process must consider all possible options.

The following figure helps to visualize the surfaces that should remain the same in the new redesign. Despite their shape is constrained, their position is not, so these surfaces can be moved with total freedom in the space. In green the profile of valves and in blue the envelope of the interface for the connectors.

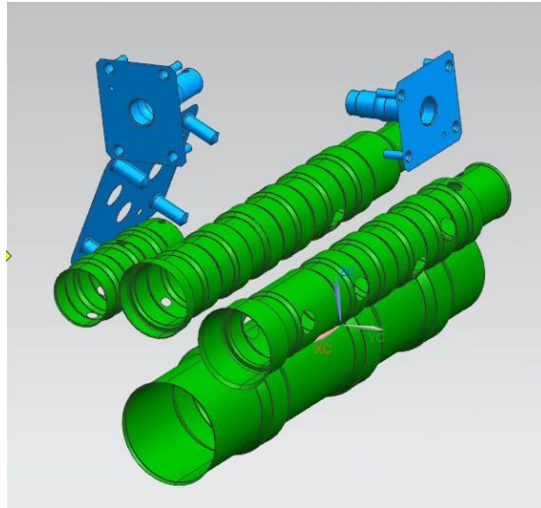


Figure 5.2 External profile of the valves and connector interfaces to maintain in the redesign.

The most relevant potential concepts for the valves layout are reported below. The rest of the schematic connections with other elements is also reported to have an overall view of the possible channel layout (it is important as well to make every connection as short as possible so analyzing how would be the resultant hydraulic circuit is also necessary to assess the feasibility of the proposal).

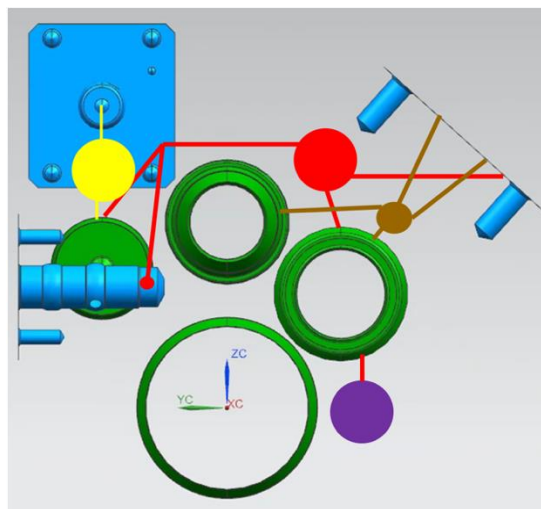


Figure 5.3 Possible conceptual layouts. Frontal view of proposal 3.

The schematized figures helped to make more rapid modifications and to think of more varied concepts without entering in the detailed design with all the constraints. All the views reported below are front views to appreciate better the distribution of elements and all of them are colored to distinguish between schematized elements. The yellow, red and purple circles represent the pump inputs, while the brown one represents the non-return valve. The most relevant hydraulic channels are showed to check the feasibility of every proposal in terms of channels. The fixed

reference in every case is the beta tube, as it is the only element that is constrained to keep the form and the position with respect to the baseline.

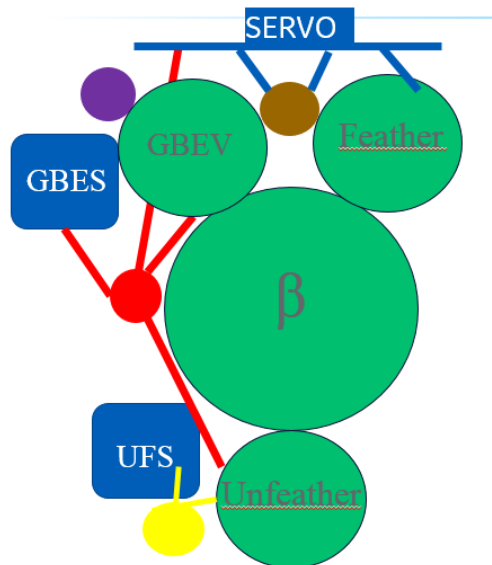


Figure 5.4 Proposal 4 for possible concept of layouts.

This proposal 4 considers the valves spaced at equal angles with the intention of sharing efficiently all the space of the front flange as it had to maintain the outer shape circular. Also, the objective of reducing the number of channels combined with the advantages of additive manufacturing implies that the connections between valves can be done directly without designing any channel for that purpose as the external material of the valves would be merged and the hole can be printed in the inside. However, the resulting channels are too long and the connectivity can be still improved. This issue is the driver of the proposal 5, where the valves are arranged closer to each other reducing the material for the conformal channels.

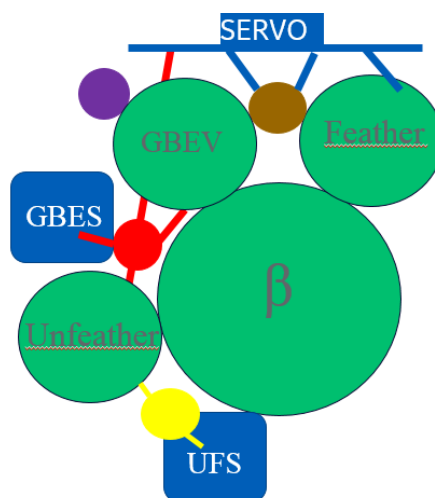


Figure 5.5 Proposal 5 for possible conceptual layouts.

Certainly, this proposal was very promising, as every element was very close to their respective connections. Nevertheless, the fact of considering the surfaces of the solenoid connectors perpendicular to the build direction was not appropriate as the connectors had a 90° elbow shape while the purple pump source was likely to be in a better place to help the proposal to be more compact.

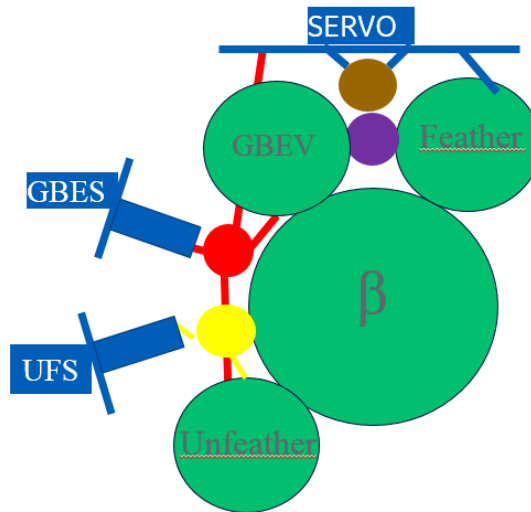


Figure 5.6 Proposal 6 for possible conceptual layouts.

All of the previous considerations were taken into account and the proposal 6 was developed. The interfaces to attach electric connectors are moved to be parallel to the build direction. Furthermore, the purple supply was moved to be between the GBEV and the feather valves to reduce the size of the external envelope.

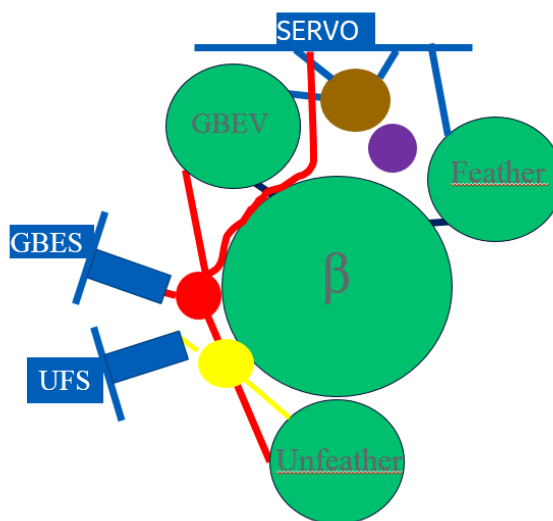


Figure 5.7 Proposal 7 for possible conceptual layouts.

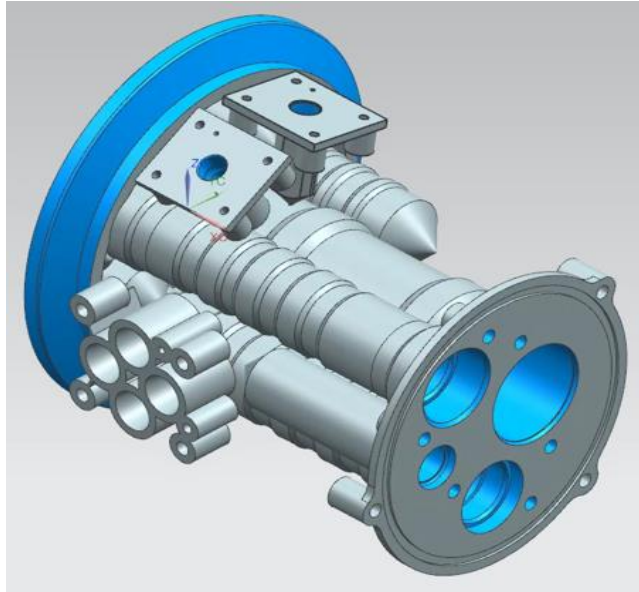


Figure 5.8 Proposal 7 3D CAD model without the wrapping shell for the oil drain sump.

At the stage of elaboration of proposal 7 it was noticed that due to assembly interference between different parts the minimum distance between valves was bigger than expected, so the black lines where added representing the channels between valves. Also, another opportunity for additive was discovered by considering the channels for oil embedded in the bodies of the valves. This has two advantages simultaneously: the length and cross section can be optimized with a complex geometry and the need for supports for printing is suppressed as the structure will be joined to a functional part saving material and printing time.

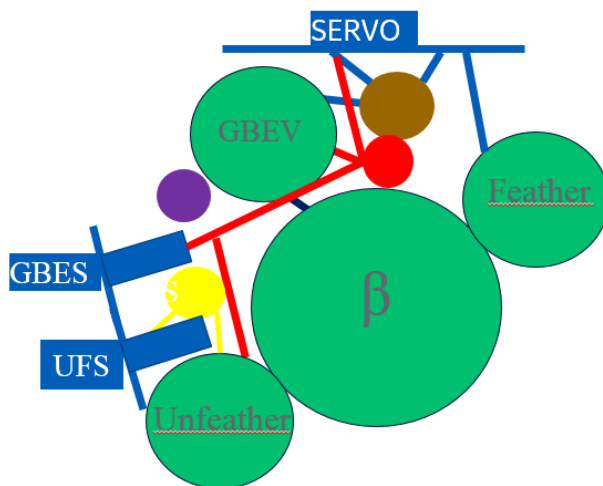


Figure 5.9 Proposal 8 for possible conceptual layouts.

As the oil lines from the red supply were not very convincing, another possibility was explored to substitute the purple supply with the red one trying to bring closer the different connections and reduce the overall length. Additionally, the connections of the yellow supply were shortened. The

feather valve finally could have the shared hole with the beta transfer tube and the unfeather valve despite not having any connection with the beta transfer tube was considered to be attached to it with the objective of increasing the stiffness of the structure.

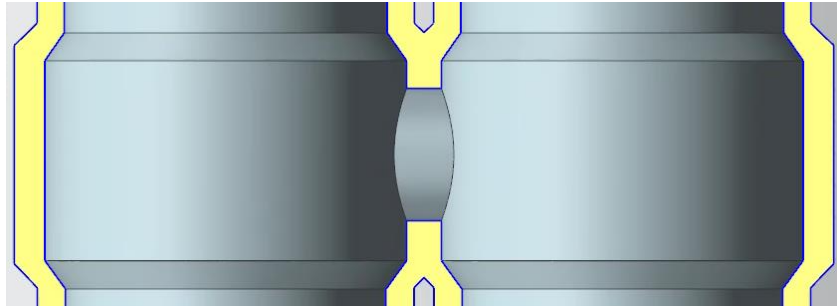


Figure 5.10 Section to illustrate the concept of shared hole directly printed within the bodies of the valves.

The next iteration for the design was very important: as the space around the beta transfer tube had to be optimized in terms of occupied volume, one beneficial modification was found by moving one of the connectors to the right side of the beta transfer tube finding more space to move not only the connector, but its pressure supply as well to the right side of the beta tube. The separation of connectors conferred more freedom for their orientation with respect to the servo valve, a fact that was harnessed to fulfill the design driver of orientation of connectors for assembly.

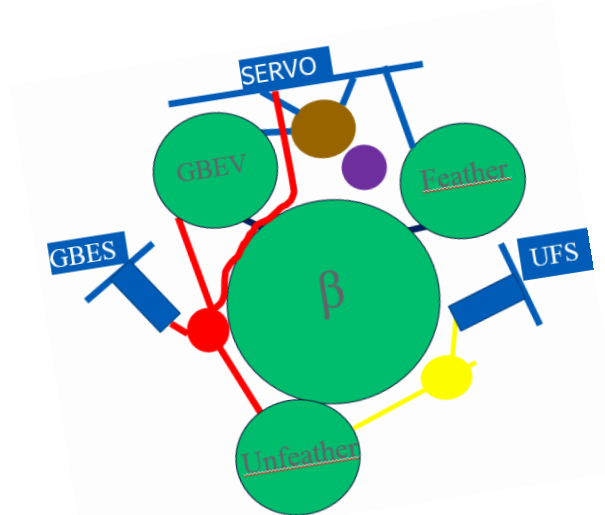


Figure 5.11 Proposal 9 for possible conceptual layouts.

After identifying proposal 9 as very promising, it was decided to set up the CAD modeling phase to put all the elements together and check the suitability of the proposal. Unfortunately, as one of the requirements of the new design was to improve the position of the connectors to favor the assembly of the unit in the engine, this proposal was not precisely an adequate option. Therefore, another loop was necessary to find a suitable layout.

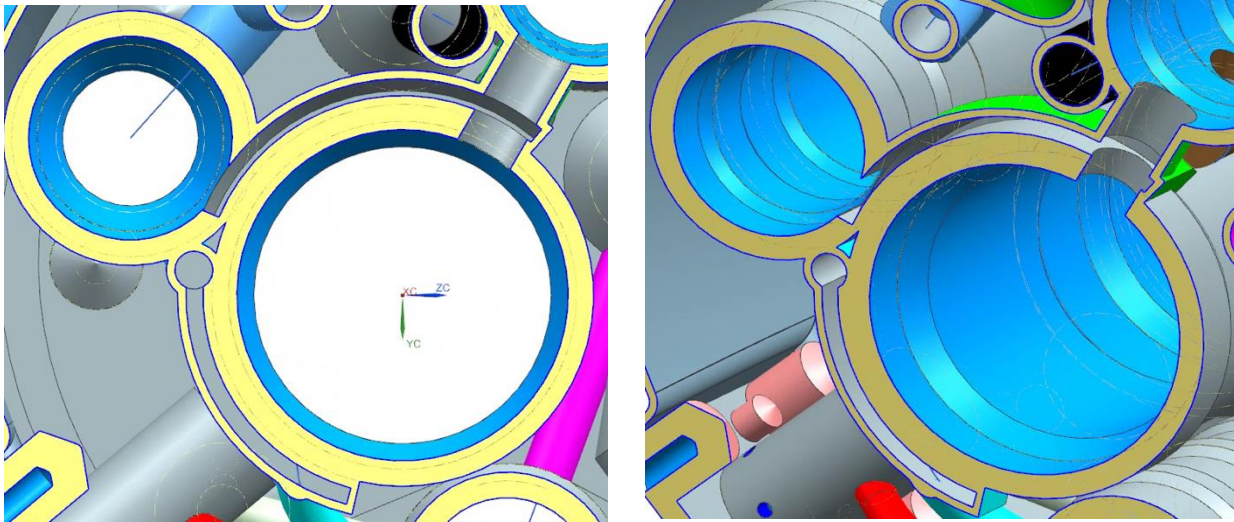


Figure 5.12 Detail of the section for some oil lines attached to the body of a valve to save printing supports.

Fortunately, the suitable option was not too far from the proposal 9, and only minor changes had to be made to it. Basically, the orientation of the connectors was rotated around 90° to distance the connector from the parts of the engine where an interference existed. Hence, the proposal 10 was found to meet all the requirements for the redesign and the preliminary design phase was considered to be finished to start with the next phase, the detailed 3D CAD modeling.

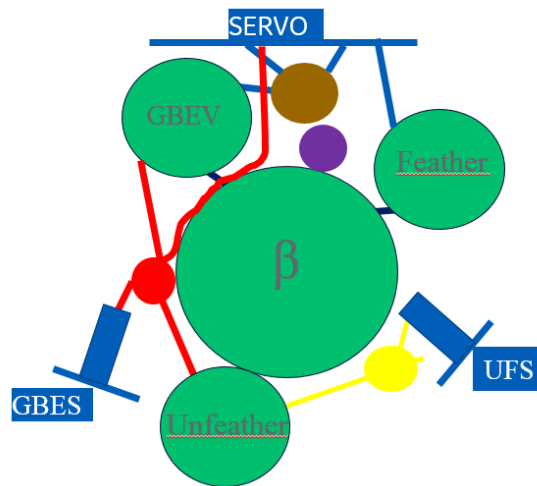


Figure 5.13 Proposal 10 for possible conceptual layouts. Definitive CAD solution adopted.

Once the optimum proposal to meet all the requirements was chosen, it was designed in detail within a 3D CAD software package to make sure in detail that all the constraints for machining and for assembly were accomplished. For instance, there should be at least 4 mm of clearance between surfaces that eventually will be machined to ensure enough material resistance during the machining.

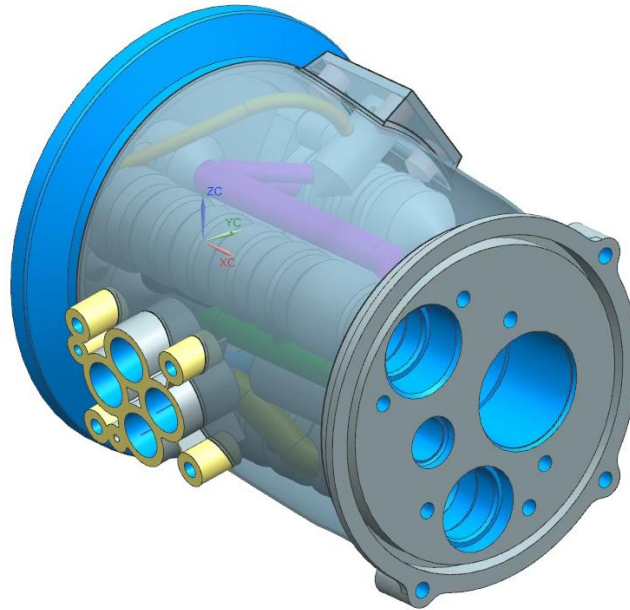


Figure 5.14 ISO view of the CAD concept.

The model is wrapped around a shell to ensure the oil sealing and simultaneously to serve as the drain sump for the draining oil. This shell is a parametric surface created by CAD and has the advantage that can literally wrap the model adapting its shape to every section of the body. The consequence of this is a complex structure, big weight saves and a more compact design, which are the perfect conditions to consider additive manufacturing to apply.

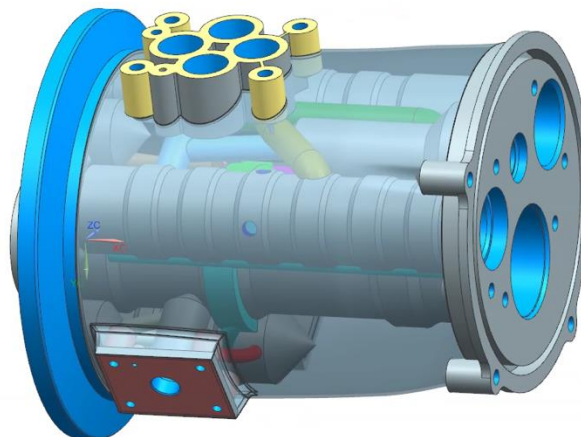


Figure 5.15 Detail of the draining of one of the valves directly to the enclosed volume by the shell.

From the ISO view it can be seen as well that the strainer plate that was used to filter the oil has been integrated to the model, introducing mass only where needed in the surroundings of the filters and bolts, creating a very tailored profile only feasible if additive is considered.

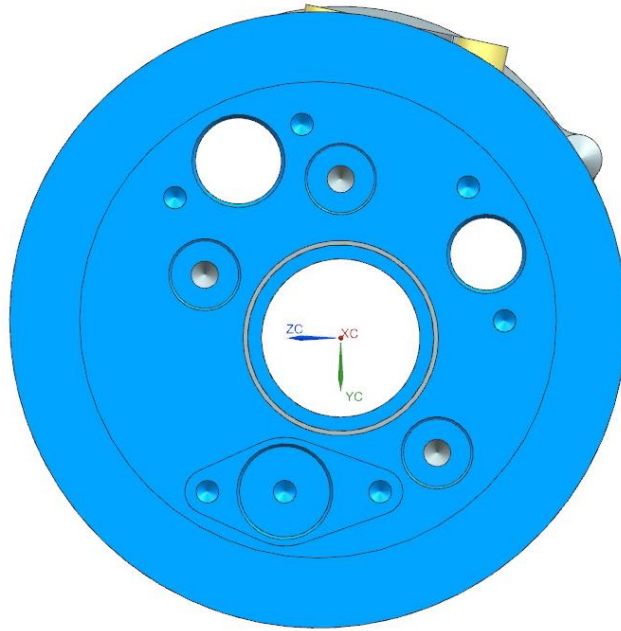


Figure 5.16 Front view of the CAD concept.

In the front view, it can be noticed that the unfeather valve is moved to the front flange to save space in the rear flange where it was attached previously. At the same time, in order to avoid interferences in the front flange during assembly with the other components, a pocket with the height of the valve cap is considered in the front flange.

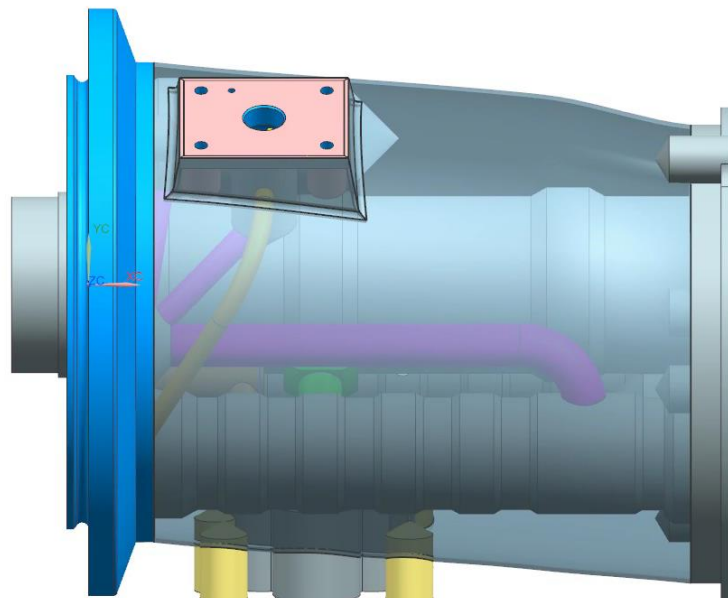


Figure 5.17 Lateral view of the CAD concept.

In the lateral view it can be seen that an eccentricity exists between the front and rear flange, forcing the shell to be modeled in a shape such that accommodates both flanges. The shell designed in this case is a preliminary concept that satisfies the requisites however it is far from the optimum shape.

Moreover, from the lateral view it can be noticed that all the connector interfaces are positioned as close as possible to the flange with the objective of favoring the design for dynamic purposes. Indeed, the consequence of this design choice would be less mass bouncing far from the clamped flange, adding less inertia to the unit when it vibrates and therefore improving the stiffness.

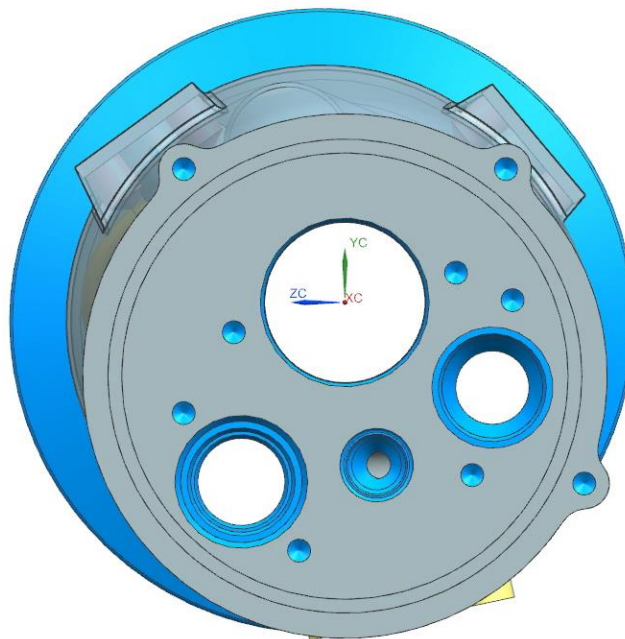


Figure 5.18 Rear view of the CAD concept.

In the rear view it can be noticed that the number of bolts necessary to assemble the main body with the main housing has been reduced to 3 bolts, although it could be increased to 4 mm in case of necessity, maintaining in every case the overall reduction in number of bolts.

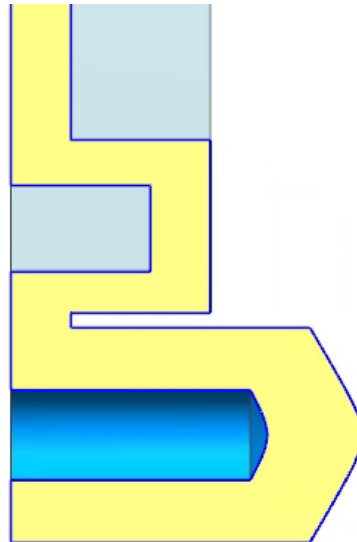


Figure 5.19 Detail of the section of the sealing radial O-ring solution adopted.

The profile of the rear view has been chosen with a circular section to exploit the use of rubber circular O-rings to seal the interface between main body and mid housing, providing a simpler and more standardized solution for this issue. Afterwards, the decision had to be taken if to use or a radial or an axial sealing O-ring. The axial O-ring is presented in fig 5.20, while the radial version is presented in fig. 5.21. Eventually, the radial O-ring installation was chosen, in particular the version of the left side of the figure 5.21 because it is the solution for the static case incorporating bolts for the installation of the mating parts. The reasons to do this were because it was cheaper, easier to install and more reliable solution than the axial version. Moreover, the engineering experience in industry demonstrates that this is the right solution. Nevertheless, it has to be remarked that the axial version for the O-ring is still perfectly valid from a designer point of view and should work as good as the radial one.

Axial installation, static

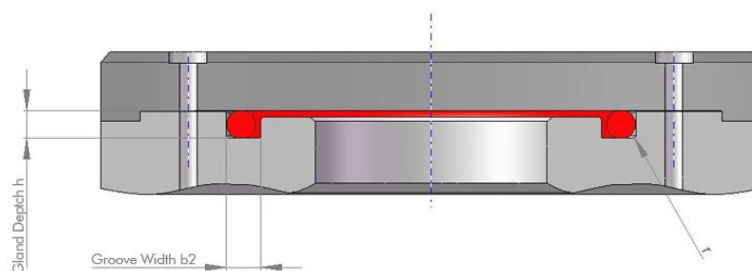


Figure 5.20 Axial sealing O-ring option.

Radial installation, static and dynamic

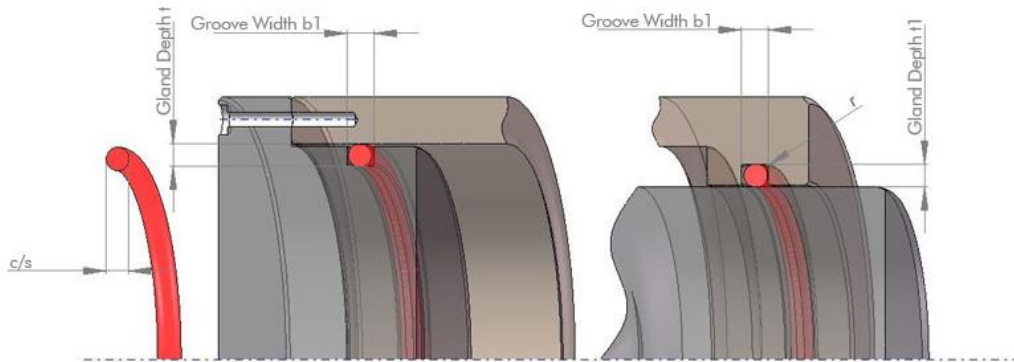


Figure 5.21 Radial O-ring to seal the interface between mid-housing and the main body. A variant of first option was adopted.

The minimum distance between valve caps once assembled is chosen to be around 2-3 mm for assembly clearance reasons.

It was necessary to set the minimum distances to give the post process tooling a certain margin to machine the surfaces in the post processing. The minimum distance in the frontal plane between the pump supplies and the beta tube machining was chosen to be 5 mm, due to the criticality of this part of the component. On the other side, for the rest of machined profiles the minimum distance in the plane between them was set to 3 mm.

The thickness chosen for all the holes is chosen depending on the material, but a conservative choice of 3 mm was taken to avoid problems during the building process and to support the operating range of pressures at which the component is supposed to work.

Additionally, the tooling allowance for subtractive operations such as milling and machining was considered to be 2 mm and applied to all the interfaces that would be machined or milled after the printing to ensure finishing requirements, e.g. bolt drillings and valve profiles.

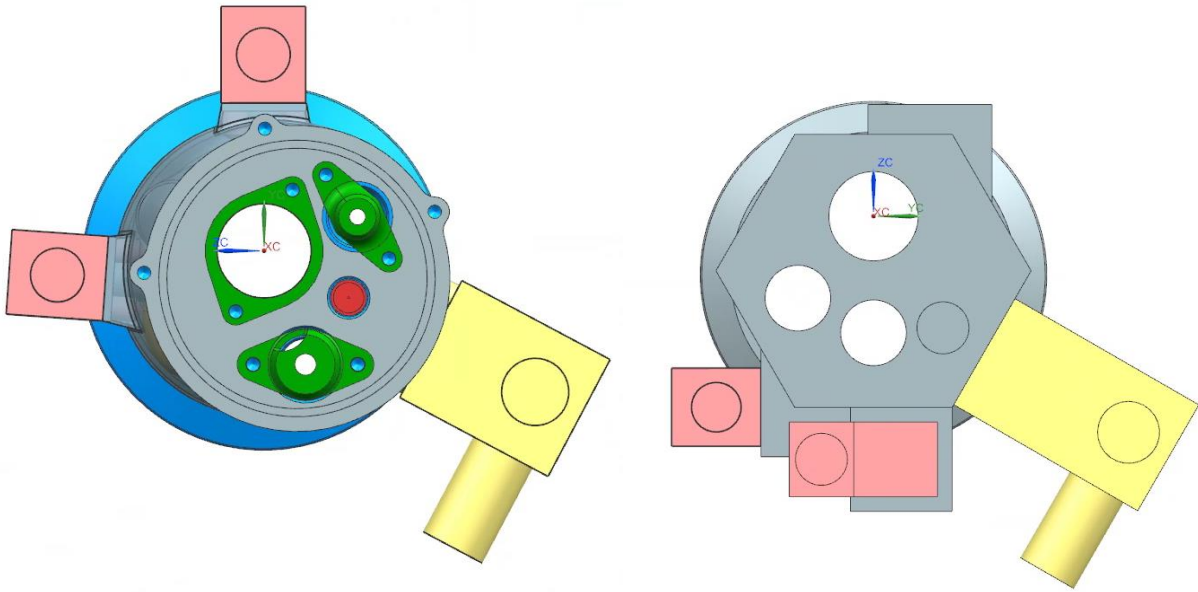


Figure 5.22 Final CAD solution adopted. Notice the new position of connectors to improve engine assembly operations.

5.2. FEM analysis

The main objective of this step is to optimize the frequency response of the PCU body by measuring the misalignment of the beta transfer tube axis. The frequency range of external excitation is given by the certification standard vibration test, and the input loads are measured in acceleration units, as well as the output response from the system.

Additionally, the misalignment of the axis of the beta transfer tube is monitored to assess possible malfunction of the system to transmit command to the propeller.

5.2.1. Baseline analysis

In this section the dynamic analysis of the baseline carried out in the dummy model created to schematize the real component is discussed and compared to the results of the main body of the baseline. Then, the validation of the dummy model is discussed by comparing the results obtained. The results will be given in terms of percentages as the actual data is confidential.

The data shows that the approximation can be acceptable in terms of dynamic analysis as the frequencies of modes and the modal participation factors as well show that the deformed behavior is equivalent, especially when the dummy model does not take into consideration the complexity of drillings and the external shape is roughly approximated. In conclusion, the dummy model can be a substitutive model for dynamic calculations instead of the complex main body of the baseline especially indicated for the simplicity of the meshing.

Number of mode	Difference in the modal frequency with respect to baseline, in %
1	+13.2
2	+10.45
3	+9.28
4	+2.77
5	+4.23
6	+7.49
7	+6.12
8	-2.62
9	+1.57
10	+1.78

5.2.2. Dynamic analysis approach

As the original design was projected and certificated before the structural software tools were developed, it was necessary to find an equivalent approach to model the loads applied to the component. As a vibration test was performed to certify the original structure this test was identified as one of the most restrictive conditions. The test was performed using a shaker table where the body was fixed and subject to certain dynamic conditions. To model this behavior, two approaches were followed:

- Take the shaker table as the absolute reference frame and apply the acceleration input in the three directions of the space to all the nodes of the body, simulating the inertia of the body when it is shaking. The degrees of freedom of the nodes in the clamp are all constrained to be zero as they move rigidly with the base. An explanatory schematization of the approach can be found in fig. 5.23.

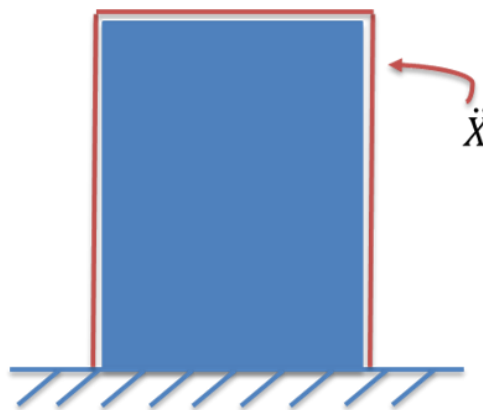


Figure 5.23 Shaker table as the absolute reference.

- Take an external absolute reference and consider the shaker table as a mobile reference. In this case, the imposed acceleration input is applied only to the nodes clamped to the table fixture, leaving the rest unconstrained with free response. Indeed, this is the most immediate model that one can think about when it comes to modeling these conditions. The schematization of this approach is depicted in fig. 5.24.

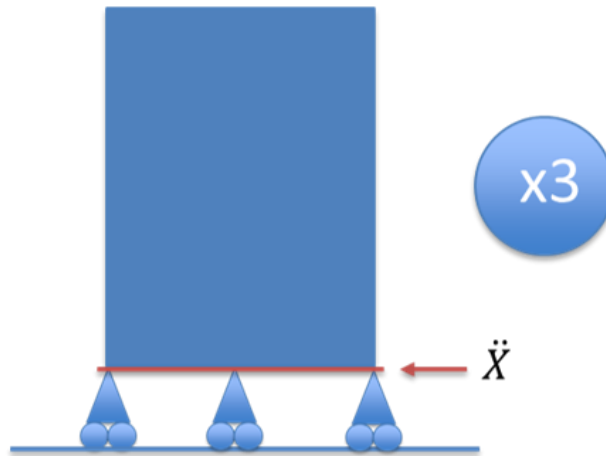


Figure 5.24 External non- inertial absolute reference.

5.2.3. Topology optimization

Subsequently, this analysis in every three directions of space is used to apply the loads to the structure and will be the main driver of the topology optimization. It has to be noted that the covering shell was removed in this stage to allow more freedom for the algorithm to add or subtract material in the space. Obviously, once obtained the results, the body should still be wrapped around with a shell to allow draining from the valves. However, this shell will have the difference that will have no structural responsibility and therefore the thickness for this element can be reduced to the minimum available by the process to minimize the total mass. The resulting non-design space with these conditions is depicted in fig. 5.25.

Moreover, the analysis of the frequency response of the body is crucial in this phase because if the beta tube axis misalignment at a certain frequency exceeds some certain value, the operation of the unit might be compromised and therefore the performance of the whole engine.

In addition, the fact of optimizing a dynamic case was considered of particular interest for the company. To model the loads, it was necessary to understand the method to implement them properly in the FEA software. More information about the implementation of these conditions in the FEA software used can be found in the Appendix A at the end of this thesis work.

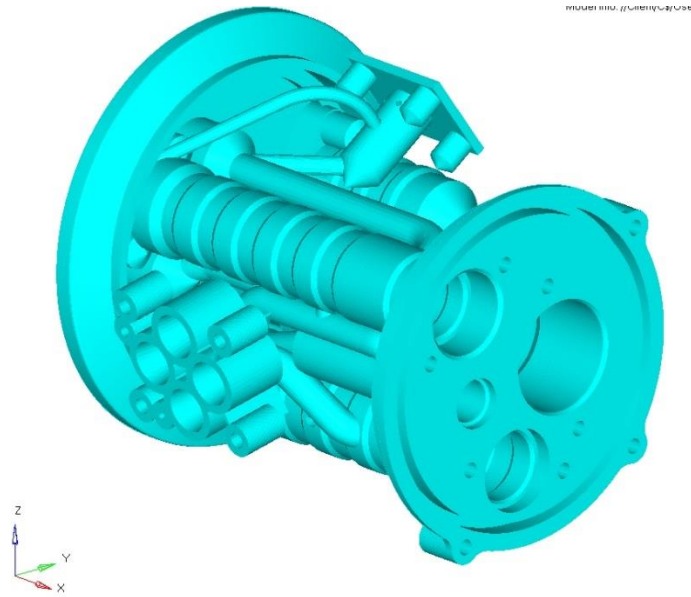


Figure 5.25 Non-design space meshed.

The choice of the design space was an iterative process where a tradeoff between computational time, convergence and quality of mesh was needed to be made in order to find the most adequate configuration to launch optimizations in a relatively fast and at the same time reliable way.

- Design space: version 1

The first design space was taken as a conceptual design space with some volume margin to avoid the loss of information coming from the solver to some load path. However, this design space was discovered to be unsuitable for excessive computational time and excess of memory space occupied.

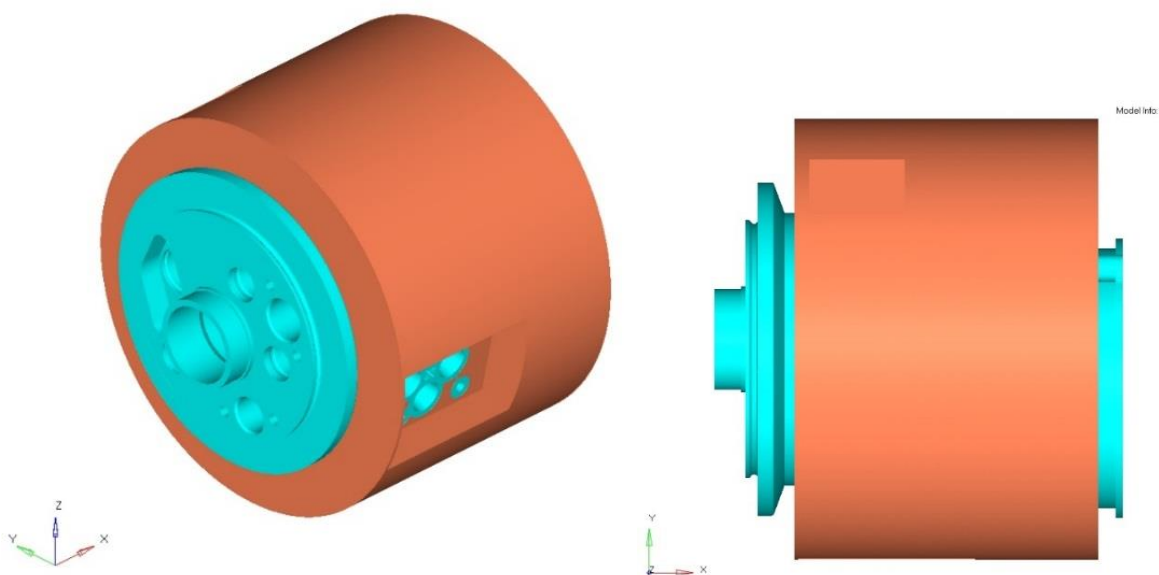


Figure 5.26 Design space version 1.

- Design space: version 2

The second version of the design space was made to be smaller in the radial dimension, which saved memory and computational time. At the same time, it was noted that the design space should respect the envelope of all the components assembled together, i.e. the interfaces with connectors, with the consequent volume restriction for the volume. However, this design space was still heavy in terms of memory and the convergence of the optimizations was still very low, in the order of days.

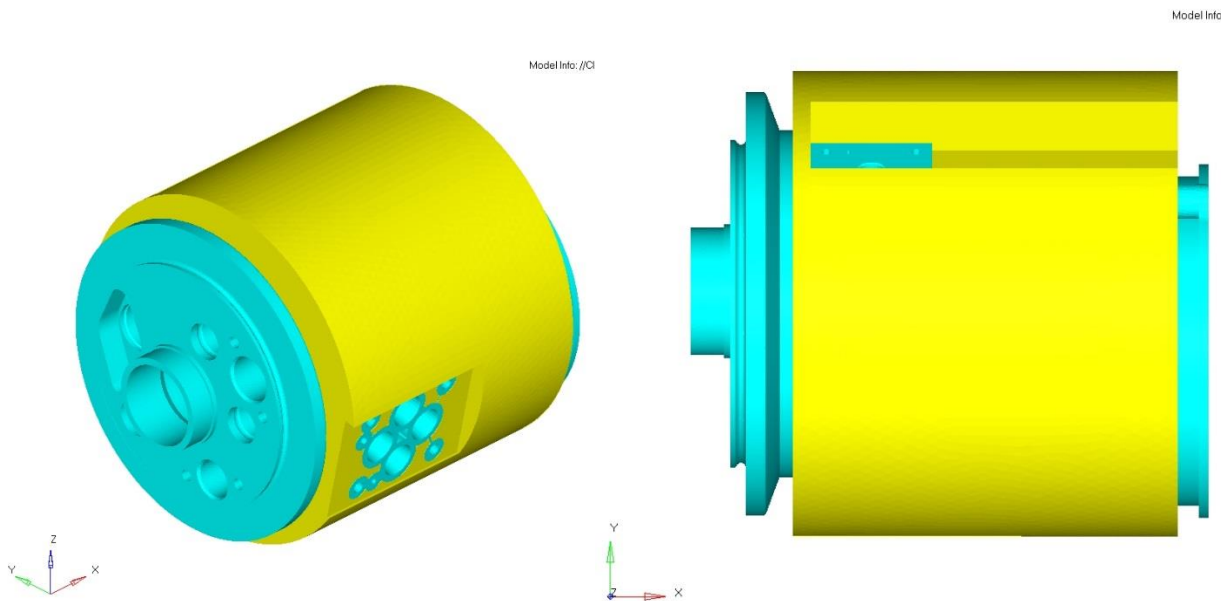


Figure 5.27 Design space version 2.

- Design space: version 3

For the third iteration for the design space, the modifications of the second version were kept while the radial dimension was even more reduced. The most relevant new feature in this version of the design space was the tangential attachment to the non-design space to favor the following smoothing process. Also, it was decided to consider that between these attachments and the maximum envelope of the design space, a manufacturing constraint of 45° for the overhang angle, which is the theoretical maximum overhang angle for printing so that the resulting optimization will respect this manufacturing constraint in every case at least for the main resulting structure and attachments to the non-design space, simplifying the smoothing and the geometry reconstruction.

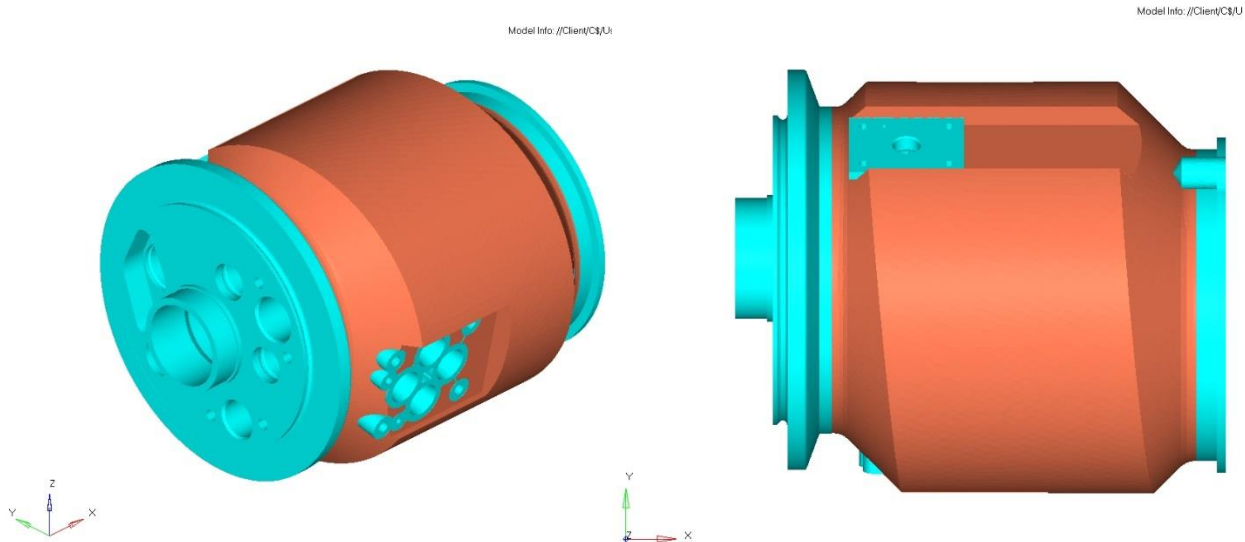


Figure 5.28 Design space version 3 with the edges at 45°.

A summarizing table with all the data of the design space versions can be found in table 5.1.

Design space version	No. nodes	No. elements	Mass (%)
1	1242954	7019385	100 %
2	160004	905303	63.15 %
3	177294	895997	49.64 %

Table 5.1 Design space mass and FEM characteristics.

5.3. Optimizations

In this section the different optimizations carried out are presented. The values obtained depend strongly on the optimization parameters chosen before launching the solver. Some of those parameters are presented below.

- MINDIM: specifies the minimum diameter of members formed in a topology optimization. This command is used to eliminate small members to avoid unconnected domains. The recommended minimum value for this parameter is three times the dimension of the element of the design space mesh.
- DESMAX: maximum number of design iterations. When the MINDIM parameter is active the default passes from 30 to 80.
- CHECKER: this is a 0 or 1 parameter, and activates or not the checkerboard-like scanner for elements. The undesired effect is that a layer of semi-dense elements will remain at the transition from solid to void. It is recommendable to activate if the parameter MINDIM is also fixed.
- DISCRETE: is an equivalent parameter for the penalization parameter of the SIMP method. The higher the value of this parameter, the more aggressive is the penalization. This

parameter controls the optimization for densities to take a discrete value between 0 and 1.

Both DISCRETE and p parameter are related by:

$$DISCRETE = p - 1 \quad (5.1)$$

- MATINIT: sets the initial material fraction of the design space.

5.3.1. Min mass with lower bound in first mode frequency

It was discovered that one of the variables that had more influence in the response of the solution was the frequency of the first mode. Indeed, if the optimization objective is to minimize mass, the solver will try to do so, but decreasing the stiffness as well and therefore. The effect of doing this is not proportional, as the optimizations were showing because it could be noticed that the natural frequencies of the body were decreasing as the optimization advanced. Then, the frequency has to be controlled to avoid the natural frequencies of the body to fall in the undesirable range where the test is going to be carried out. To do so, and to follow a conservative road, the frequency at which the optimization was constrained was set to be a 15% higher than the higher frequency of the shaker test. In order to see the differences between the value of frequency chosen, two optimizations were launched: one with the constraint at the maximum frequency achieved in the shaker table vibration test and the second one with the constraint at the same frequency plus a 15% margin for safety reasons.

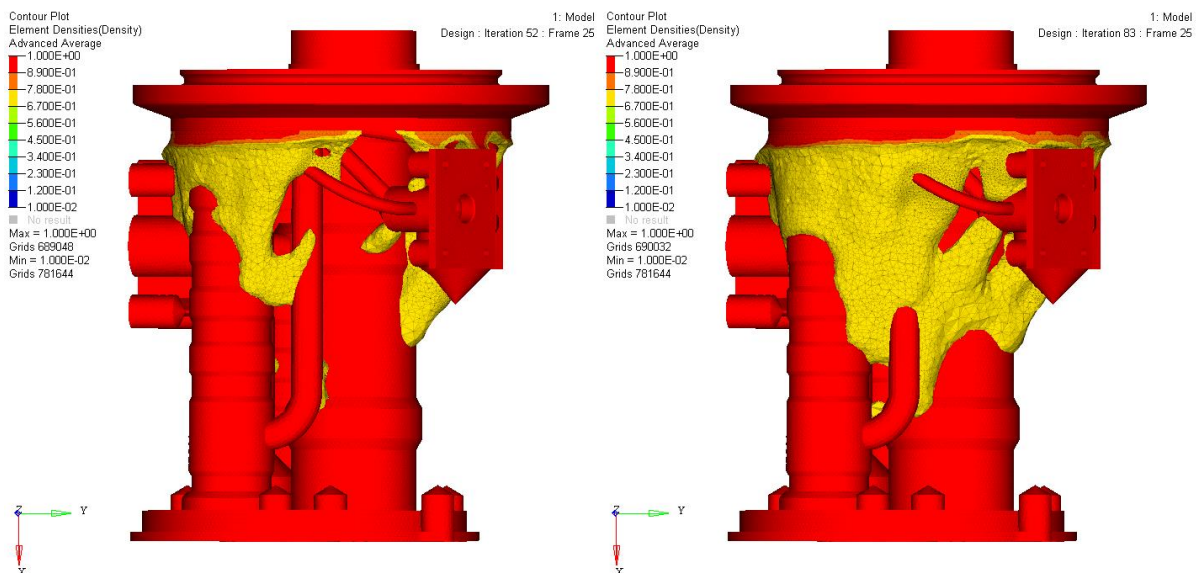


Figure 5.29 First frequency constrained to the max frequency of test (left) and the max frequency plus a 15% margin (right). Density threshold >0.7.

The results confirm that the conservative choice has more homogeneous distributed density creating better connected volumes. On the other hand, the total mass has increased but the save margin is still big compared to baseline.

5.3.2. Min mass with frf displacement control

The control has to be more exhaustive the optimization constraint range has to be smaller because if not the solution will tend to eliminate all the design space as the non-design space alone is compliant.

As always, the results that the solver was asked to monitor were the misalignment of the beta transfer tube axis by the using of RBE3 elements.

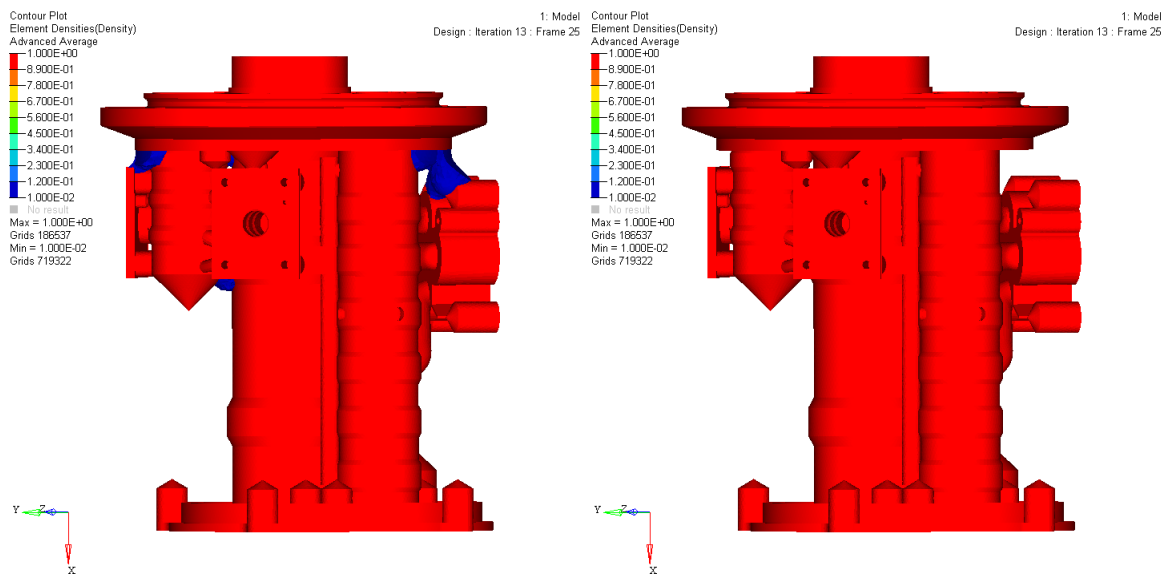


Figure 5.30 Frequency response displacements constrained to a reference value. Left: low structural damping ratio. Right: five times higher structural damping ratio.

The results show that setting a design constraint for misalignment equal to the maximum value of displacement of the main body of the baseline, the solver does not consider necessary the addition of material from the design space, i.e. the non-design space is compliant itself. Consequently, the control on displacements was considered not to be dimensioning from the point of view of the solver, or at least, not as much as the first mode frequency.

However, one interesting result can be obtained from these calculations. During the sensitivity analysis of the optimization to the value of the structural damping coefficient, it was discovered that with a default value, the optimization did not add any material to the non-design space, while when it was set to a value five times lower, the solver added some material but with a very low density (almost equal to zero) showing that the closer the optimization is to the undamped case the more

material is added. The physical explanation for this behavior is that the above a certain value of the damping the response of the displacements is inside the desired ranged.

5.3.3. Min mass with lower bound in first mode frequency + frf displacement control

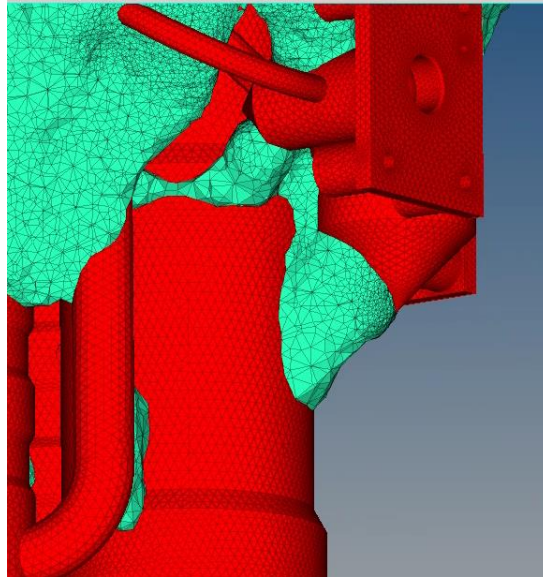


Figure 5.31 Detail of support built casually by optimization.

The resulting structures constitute a good structure layout as well for additive manufacturing, as can be seen in fig. 5.31. The attaching structures can serve as well as supports to avoid overhang situations during the process. Indeed, it can be seen that the blue added material serves as support of the red valve that previously had anything to support its build.

5.4. Smoothing & solution refinement

The results of topology optimization are rarely manufacturable directly, even by AM. This is in part because topology optimization is a technique to apply to get concept for the load paths and is important to bear this in mind. Typically, designs retain their meshed surfaces so that they are rougher than would be desired. Part regions may become unconnected or very thin between thick sections, introducing unwanted stress concentrations.

The smoothing tool included in the FEA software tool used analyses and processes the resulting elements from optimizations taking the solution from the solver and remeshing the volume to make possible a further remesh to validate the results when the threshold value for density is chosen.

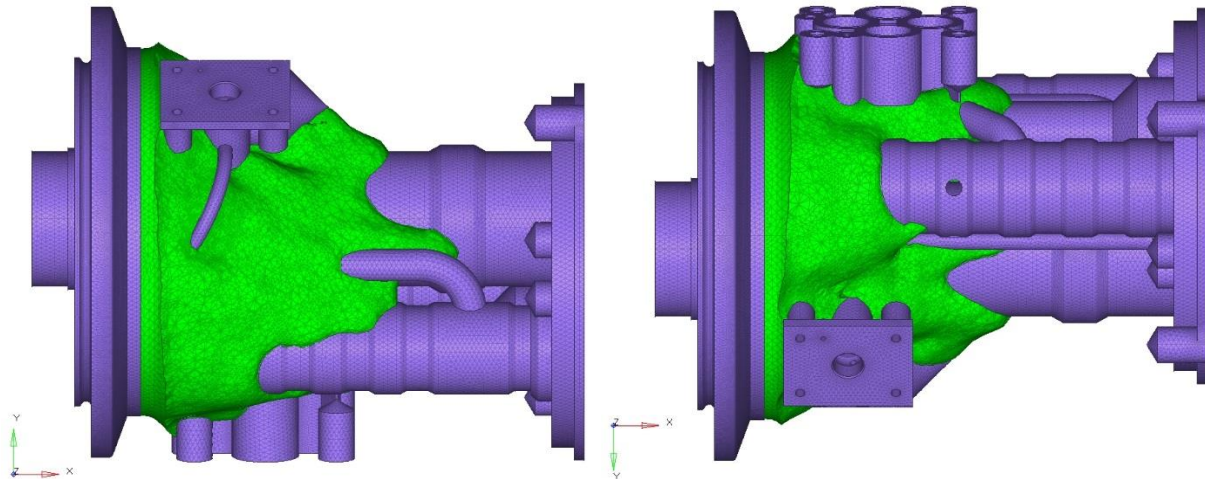


Figure 5.32 Resulting design space after the smoothing with the software tool.

The differences between before and after the smoothing process can be seen in fig. 5.33. One of the missions of the smoothing after the optimization step is to transform the geometry of the solution to an easier-to-handle 2D mesh. The purpose of this is to be able to make a regular 3D mesh with the properties of the material that will be used in the printing to calculate the final total mass and to verify that the concept is still inside tolerances from the point of view of the structural analysis.

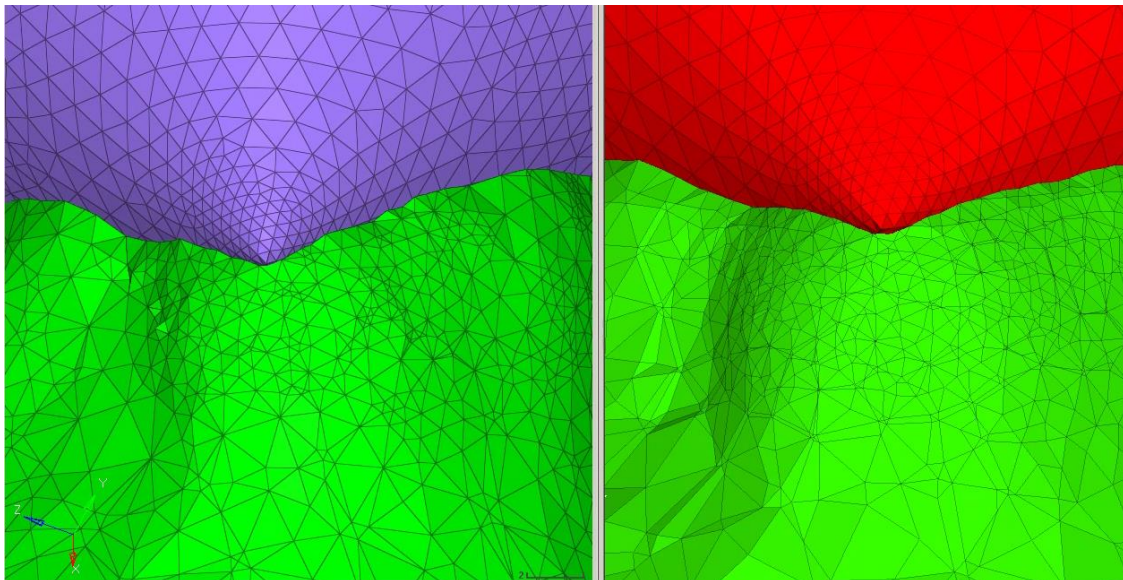


Figure 5.33 Detail of a zone before (right) and after (left) the smoothing process.

6. Design validation

As a last stage for the design process, a final validation must be done to the solution obtained from the smoothing software. This is the logical consequence of not having identically the same structure as the one obtained in the topology optimization stage. It has to be remembered that the topology

optimization has more a qualitative than quantitative character, and has the goal of identifying the load paths for a certain set of load conditions. Therefore, once obtained the structure that is likely to be printed, it has to fulfill the same requirements as the topology concept with the same set of loads when it was obtained.

The obtained solution of section 5.4 has been taken as an example to verify the requisites. After the smoothing it was remeshed to have a nice mesh to capture all the physical behavior and a modal analysis was run, giving the results in the table below. It can be noted that the fact of considering all the element solid has increased the stiffness of the structure, increasing the values of natural frequencies even more away from the threshold value initially fixed. On the other hand, the total mass was increased a 7.5% from the first to the second case, but it can be considered still a feasible solution for optimization.

Mode number	Natural frequency respect to the safety margin frequency (%)
1	+11.1%
2	+15.6%
3	+26.3%
4	+53%
5	+59.6%

Table 6.1 First five natural frequencies of the optimized concept with respect to the baseline.

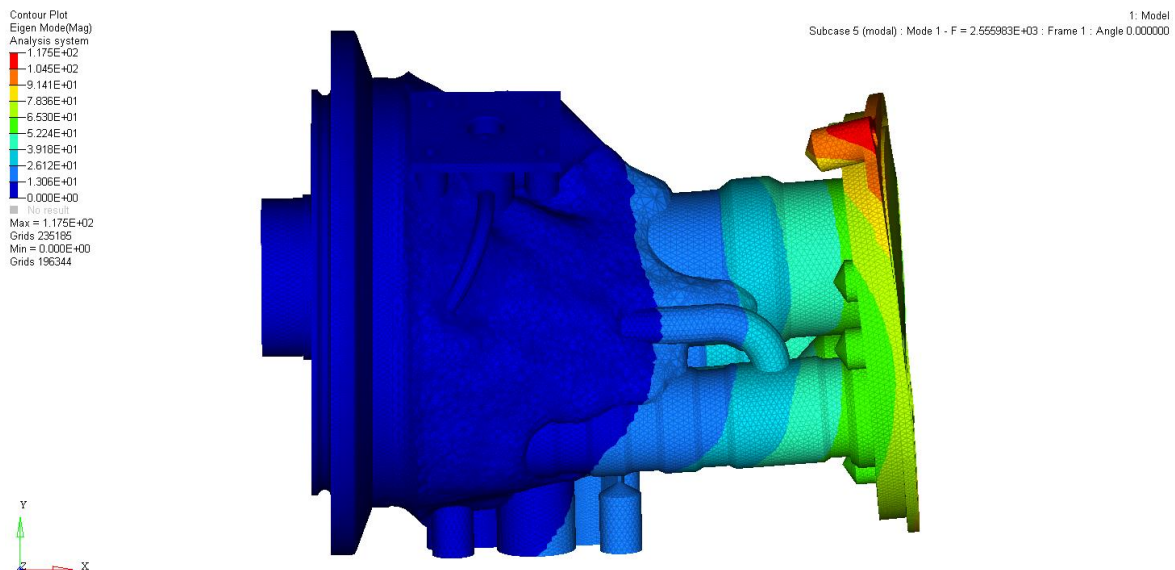


Figure 6.1 First modal deformed shape of the optimized concept

7. Further developments

As this is a case in where the component to redesign has complex functions and therefore complex geometry, it was difficult to propose modifications to the current design. However, thanks to the consideration of AM, the opportunities of improvement this component are very big and the probabilities of successful evolutions very high.

For the next iterations, a parts integration could be considered especially in the case of the assembly of the spool valves, where the assembly tolerances should be assessed to make sure that it would be enough to assemble just the spool without the sleeve, which would be integrated in the printed body saving the total number of parts. If this could be effectively done, the integration of some of the caps into the main body could be considered as well.

The control of the misalignment of the beta tube axis could be made along the whole axis through the DRESP2 card which defines an equation as a design constraint. The equation could constraint the displacement of node to be inside a sphere of a certain radius, and by applicating this equation to a set of nodes belonging to the axis of the beta tube the control could be applied in a better manner.

The business case assessment will determine the success of AM for this case study. AM is currently favored in small production lots in which the higher cost of AM specific raw materials is offset by a reduction in fixed costs associated with conventional manufacturing. Trials printed in laboratory should give the answer to this question to conclude if the new concept is feasible from the economic point of view.

8. Conclusions

In this chapter, some conclusions are made after the whole design process carried out in this thesis work. It is clear that after the selection of a part the re-design is not limited to the conventional criteria. The view has to be broadened and all functions and properties have to be taken into account. With the capabilities of additive manufacturing a significant increase in performance was realized while this was not possible with the subtractive manufacturing technologies. The freedom of design enables the designers to leave the beaten tracks and to find new and creative solutions. All the margin left for the increase of complexity has been exploited to optimize the design as much as possible.

Topology optimization should be seen as a tool in the design process that is useful to generate an efficient design concept that can be used in the early stages of the design process. The result from the topology is far from a finished product. A considerable amount of work is required to transform the concept into a finished product.

Furthermore, the performance of the hydraulic block should see an improvement because of the absence of unnecessary drillings and plugs, and as a result of smoother geometry of the internal channels. At the same time, the total weight has been reduced without penalizing too much the stiffness, which leads to a potential fuel saving for the engine. Also, the initial estimations show that the lead time for manufacturing could be reduced with respect to the original baseline, harnessing the ability of additive manufacturing of printing more than one component simultaneously. This stage of the project should be assessed deeper, though.

I. Appendix A: Dynamic analysis of a beam with imposed acceleration.

To understand better the modeling of the dynamic loads in the shaker table, a dummy model was analyzed to validate the correctness of the boundary and load conditions for different approaches followed.

For the sake of simplicity, a finite element model of a beam fully clamped in one tip is taken to assess the results from the analysis. Additionally, it is very helpful fact that this problem has an analytic solution to confront the results with.

The objective is to impose an acceleration input with a periodic law with constant amplitude (1 g) and variable frequency and monitor the acceleration response in the clamp and in the free tip in the frequency domain.

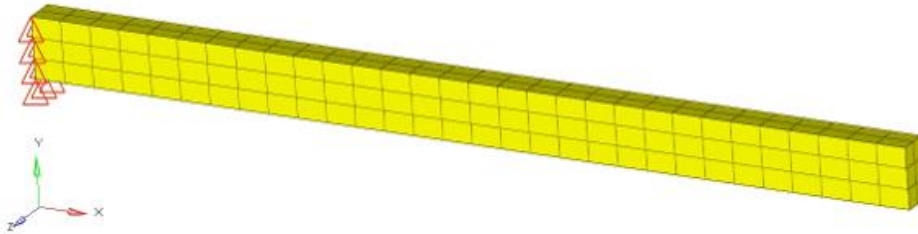


Figure I.1 Clamped beam model analyzed.

Two different approaches can be followed in this case depending on the reference frame chosen to launch the analysis.

The first one is to consider the shaker table as the absolute reference and apply the acceleration input to all the nodes of the beam to value the acceleration output relative to the shaker table reference afterwards. This is made through the RLOAD2 card in Optistruct, which defines the dynamic load and needs as input the amplitude, the frequency range and the type of excitation (load, displacement, velocity or acceleration). The acceleration is implemented through the GRAV card, noting that the solver considers automatically the load as an acceleration and therefore the distinction does not need to be made. The nodes in the clamped tip are fully constrained as they move rigidly with the shaker table fixture.

The second one consists in considering an independent external absolute reference while the shaker table is vibrating, and therefore monitor the absolute acceleration of the tip of the beam. This is made as well in Optistruct through the RLOAD2 card, but this time when it comes to applying the imposed acceleration to some certain nodes the SPCD card has to be used selecting the desired nodes and constraining them by applying the desired input of acceleration. Another condition that

the SPCD card has to satisfy is the fact that all the referenced degrees of freedom in the SPCD card have to be associated to the same degrees of freedom in an independent SPC card. Certainly, the solver will detect this condition automatically and will overwrite the SPC nodes to transform them into SPCD nodes suppressing the possibility of over constraining accidentally the model. Moreover, the load type in the RLOAD2 card has to be set this time to ACCE to specify the type of load. The constrained degrees of freedom are the two translations in the perpendicular plane to the direction of the application of the acceleration.

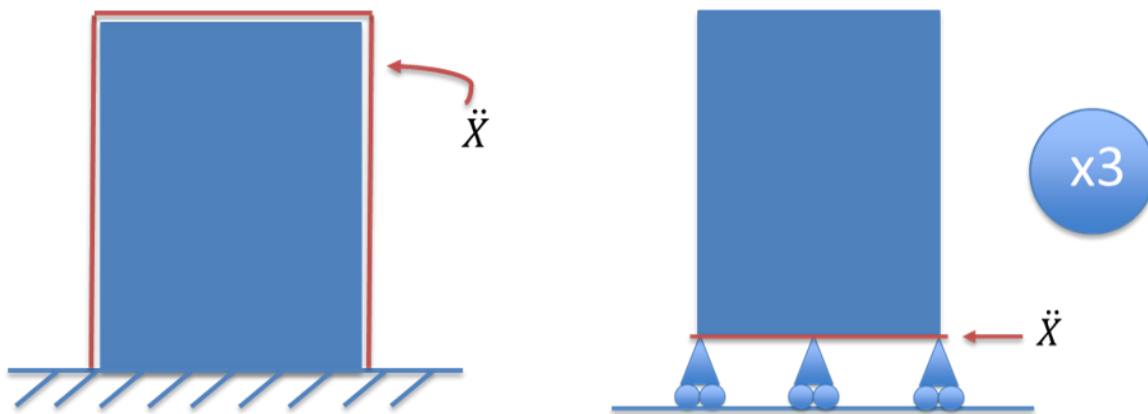


Figure 1.2 GRAV (left) and SPCD (right) approaches schematized.

In the phase of validation, the results obtained confirm that both approaches are equivalent to calculate the acceleration response in the domain of frequency. The monitored nodes were at the clamp and at the tip of the beam. In the figure below, the acceleration response for the clamp node in the GRAV approach is reported, showing that effectively the response is equal to zero as all the degrees of freedom are constrained.

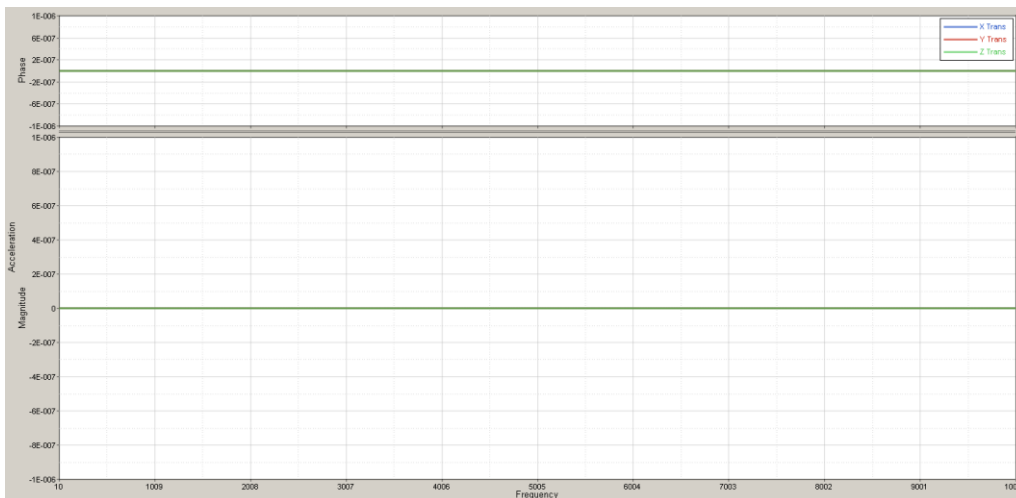


Figure 1.3 GRAV approach. Acceleration response measured in the clamp of the beam.

On the other hand, the results obtained following the SPCD approach show that the acceleration in the nodes of the clamp is equal to the acceleration imposed and does not vary with the loading frequency as the monitored node moves rigidly with the base.

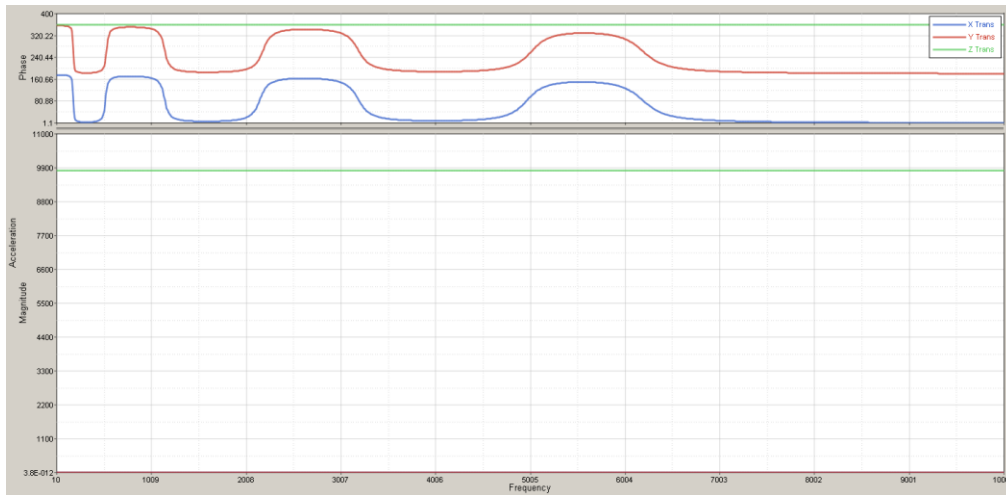


Figure I.4 SPCD approach. Acceleration response measured in the clamp of the beam.

In the case of the node at the tip, the results confirm that both approaches are equivalent to monitor the response of the non-constrained nodes. Indeed, not only the peaks coincide at the same frequencies, the values of the responses in the peaks differ in less than a 2%, considering the results as satisfactory.

GRAV	SPCD
Constrain all nodes of the base	Define the constraints (SPC) + dofs to apply SPCD constraint
Define GRAV card for all nodes of the model	Define apart SPCD constraints for nodes at clamp
Dynamic RLOAD2 type set to LOAD	Dynamic RLOAD2 type set to ACCE
Nodes at clamp response: 0 (all clamped)	Nodes at clamp response = input acceleration

Table I.1 Summarizing table with the particularities of each approach.

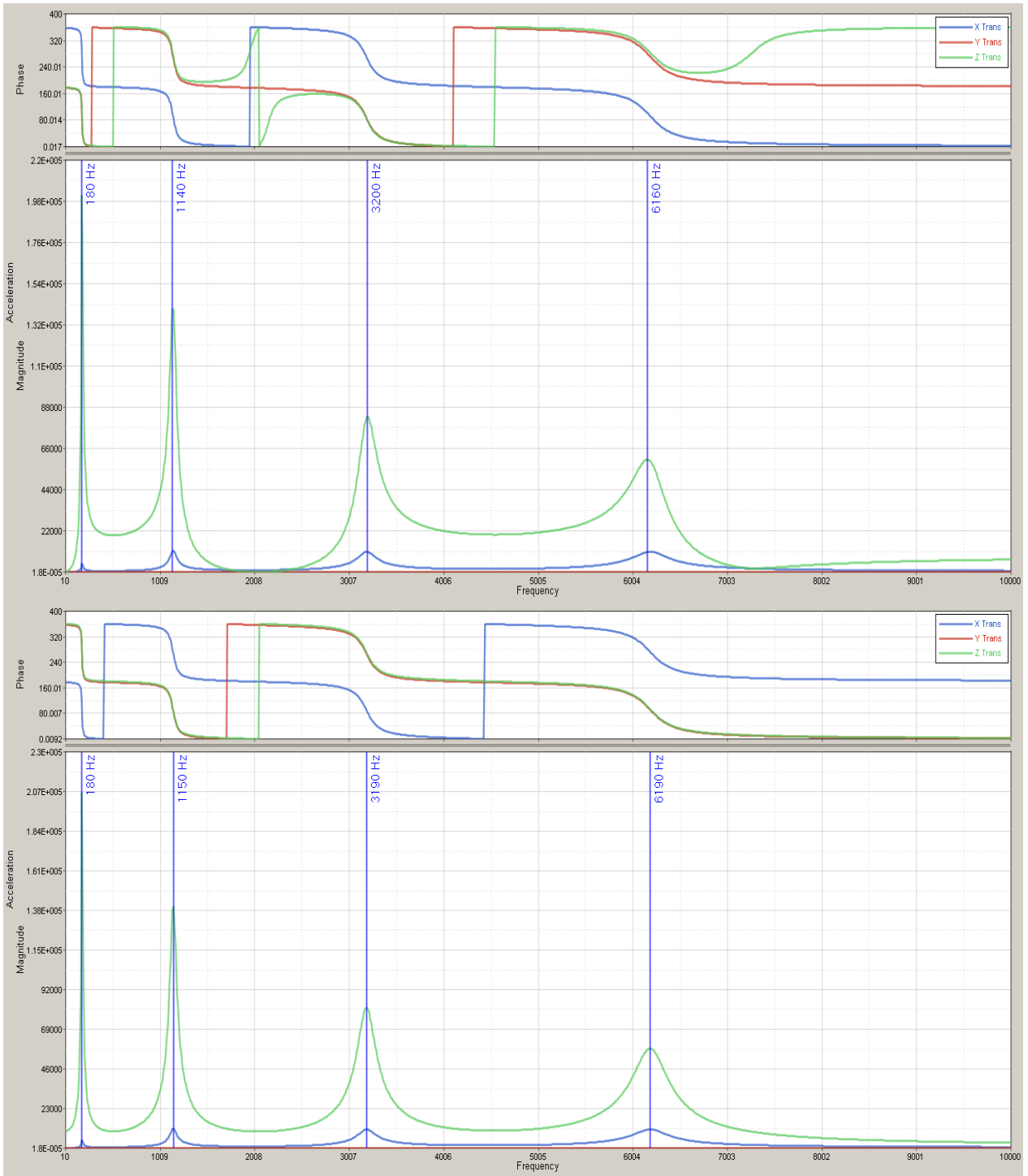


Figure I.5 GRAV (top) and SPCD (bottom) approaches. Acceleration response (magnitude and phase) measured in the tip of the beam.

II. Appendix B: Equivalent self-supporting cross section

One of the many advantages of additive manufacturing that makes the difference with respect to conventional manufacturing is the freedom to choose the geometry of the cross section that is going to be used for conformal channels without almost any restriction. Within the most interesting geometries the self-supporting sections can be considered as the best candidates to exploit in additive manufacturing due to the material saving and time savings in the printing and in the post process of the part.

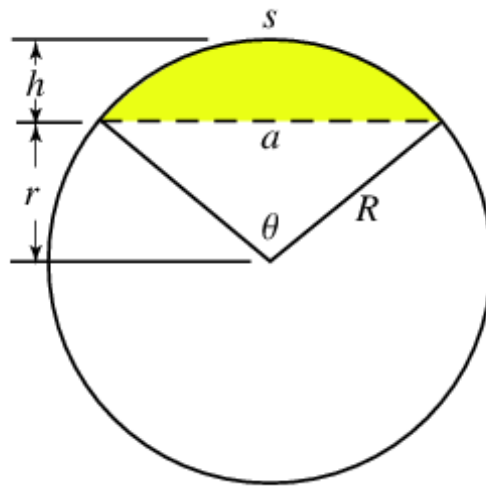


Figure II.1 Sketch for the definition of geometric parameters.

However, there can be some applications in where the area cross section should be maintained because flow rates reasons or overall capacity of the hydraulic circuit. For this reason, it is convenient to develop an analytical equivalent geometry keeping constant the area of the cross section taking some certain parameters as independent variables.

From fig. II.1, the radius is,

$$R = h + r \quad (II.1)$$

The arc length is

$$s = R\theta \quad (II.2)$$

The height r is,

$$r = R \cos\left(\frac{1}{2}\theta\right) \quad (II.3)$$

And the length of the chord is,

$$a = 2R \sin\left(\frac{1}{2}\theta\right) \quad (II.4)$$

From elementary trigonometry, the angle theta obeys the relationships

$$\theta = \frac{s}{R} \quad (II.5)$$

The area A of the shaded segment is then simply given by the area of the circular sector (the entire portion of the circle) minus the area of the bottom triangular portion,

$$A = A_{sector} - A_{isosceles\ triangle} \quad (II.6)$$

Plugging in gives

$$A = \frac{1}{2}R^2(\theta - \sin(\theta)) \quad (II.7)$$

The area of the isosceles rectangle triangle formed by the chord and the tangent sides of the arc is:

$$A_{triangle} = \frac{a^2}{4} \tan \frac{\theta}{2} = R^2 \sin^2\left(\frac{\theta}{2}\right) \tan \frac{\theta}{2} \quad (II.8)$$

And the area of the circle is obviously:

$$A_{circle} = \pi R^2 \quad (II.9)$$

Thus, the effective are of the teardrop section can be calculated:

$$A_{eff} = A_{circle} + A_{triangle} - A = \pi R^2 + R^2 \sin^2\left(\frac{\theta}{2}\right) \tan \frac{\theta}{2} - \frac{1}{2}R^2(\theta - \sin(\theta)) \quad (II.10)$$

, an expression that has as independent variables the radius of the circle and the angle theta. The latter is related to the maximum overhang angle of the material. Therefore, if one has the effective cross section of the hole and wants to pass to the teardrop concept, the new radius of the circle will be:

$$R = \sqrt{\frac{A_{eff}}{\pi + \sin^2 \frac{\theta}{2} \tan \frac{\theta}{2} - \frac{1}{2}(\theta - \sin \theta)}} \quad (II.11)$$

Furthermore, in order to avoid stress concentrations in the sharp edge of the teardrop, a fillet radius must be chosen although always the minimum available to let the area be as closest as possible to the value of the desired effective area.

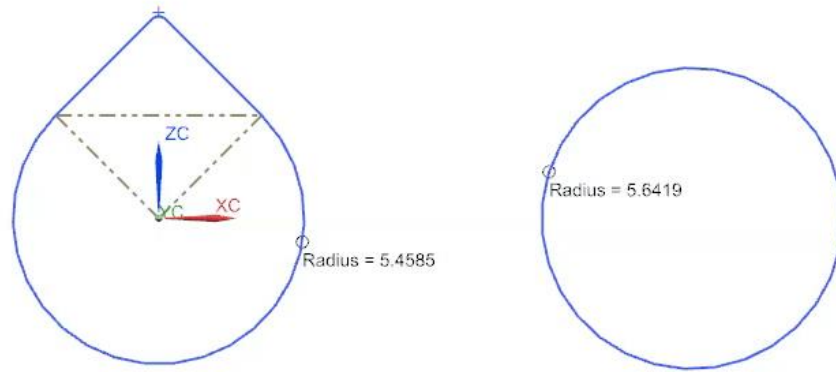


Figure II.2 Difference of radius between sections with the same area. Left: teardrop; Right: circular.

One example of an equivalent cross section can be found in fig. II.2, with the radius of the rounded parts reported. The cross-section area was chosen to be 100 mm², respected by both sections but with a small change in the local radius. The difference is almost imperceptible, but when it comes to manufacturing it can be crucial.

Bibliography

- [1] M. Hovilehto, L. Jokinen, P. Holopainen, A. Salminen and H. Piili, "Design of a hydraulic component for additive manufacturing of stainless steel," in *9th International Conference on Photonic Technologies LANE*, 2016.
- [2] W. Frazier, "Metal additive manufacturing: a review," *Journal of Materials Engineering and Performance*, pp. 1918-1928, 2014.
- [3] I. Gibson, D. Rosen and B. Stucker, *Additive Manufacturing technologies*, Springer, 2015.
- [4] "Gartner," [Online]. Available: <https://www.gartner.com/en>.
- [5] "Sciaky, Inc.," [Online]. Available: <http://www.sciaky.com/additive-manufacturing/wire-am-vs-powder-am>.
- [6] L. E. e. a. Murr, "Metal fabrication by additive manufacturing using laser and electron beam melting technologies," *Journal of Materials Science Technologies*, pp. 1-14, 2012.
- [7] "Arcam EBM, a GE Additive company," [Online]. Available: <http://www.arcam.com/technology/products/sepectra-h/>.
- [8] "Concept Laser a GE Additive company," [Online]. Available: <https://www.concept-laser.de/en/products/machines.html>.
- [9] C. Klahn, B. Leutenecker and M. Meboldt, "Design for Additive Manufacturing - Supporting the Substitution of Components in Series Products," *Procedia CIRP* 21, pp. 138-143, 2014.
- [10] P. Minetola, "Design guidelines for Additive Manufacturing finishing," Didactic materials, Politecnico di Torino, 2018.
- [11] EOS GmbH, "Basic design rules for Additive Manufacturing," [Online].
- [12] A. Patterson, S. Messimer and P. Farrington, "Overhanging Features and the SLM/DMLS Residual Stresses Problem: Review and Future Research Need," *Technologies*, no. 5,15, 2017.
- [13] "Altair," [Online]. Available: https://www.altair.com/NewsDetail.aspx?news_id=11109.

- [14] M. Bendsøe, "Optimal shape design as a material distribution problem," *Struct Optim*, no. 1, pp. 193-202, 1989.
- [15] "Hamilton Standard Hydromatic Propellers," [Online]. Available: <http://okigihan.blogspot.com/p/hamilton-standard-hydromatic-propellers.html>. [Accessed 3 July 2018].
- [16] "The variable pitch propeller pitch variation," [Online]. Available: <https://www.heliciel.com/en/helice/helice-pas-variable.htm>. [Accessed 3 July 2018].
- [17] Lee Plugs, [Online]. Available: <http://www.theleeco.com/products/precision-microhydraulics/plugs/boss-stress/>.
- [18] O. Sigmund, "A 99 line topology optimization code written in Matlab," *Struct Multidiscip Optim*, no. 21, pp. 120-127, 2001.
- [19] K. V. Wong and A. Hernandez, "A review of additive manufacturing," *International Scholarly Research Network*, p. 10, 2012.
- [20] J. Chen, V. Shapiro, K. Suresh and I. Tsukanov, "Parametric and topological control in shape optimization," in *ASME International Design Technical Conferences and Computer and Information Engineering Conference*, Philadelphia, 2006.
- [21] Renishaw, "Hydraulic block manifold redesign for additive manufacturing," 2016.
- [22] C. Klahn, B. Leutenecker and M. Meboldt, "Design strategies for the process of Additive Manufacturing," *Procedia CIRP* 36, pp. 230-235, 2015.
- [23] C. Chua and K. Leong, 3D printing and additive manufacturing, World Scientific, 2015.
- [24] D. Bracket, I. Ashcroft and R. Hague, "Optimization for Additive Manufacturing," Loughborough University, Leicestershire, UK, 2011.
- [25] E. Komi, "Design for Additive Manufacturing," VTT, Espoo, 2016.
- [26] A. Salmi, Introduction to Additive Manufacturing. Materiale didattico, Politecnico di Torino, 2017.